

## Rochester Institute of Technology RIT Scholar Works

---

Theses

Thesis/Dissertation Collections

---

5-23-1980

# The effects of concurrent photon amplification utilizing an infrared latensification source

Mitchell D. Feather

Follow this and additional works at: <http://scholarworks.rit.edu/theses>

---

### Recommended Citation

Feather, Mitchell D., "The effects of concurrent photon amplification utilizing an infrared latensification source" (1980). Thesis. Rochester Institute of Technology. Accessed from

This Thesis is brought to you for free and open access by the Thesis/Dissertation Collections at RIT Scholar Works. It has been accepted for inclusion in Theses by an authorized administrator of RIT Scholar Works. For more information, please contact [ritscholarworks@rit.edu](mailto:ritscholarworks@rit.edu).

THE EFFECTS OF  
CONCURRENT PHOTON AMPLIFICATION  
UTILIZING AN INFRARED LATENSIFICATION SOURCE

by

Mitchell D. Feather

M.S. Rochester Institute of Technology  
(1980)

A thesis submitted in partial fulfillment  
of the requirements for the degree of  
Master of Science in the School of  
Photographic Arts and Sciences in the  
College of Graphic Arts and Photography  
of the Rochester Institute of Technology

May, 1980

Mitchell D. Feather

Signature of the Author.....  
Photographic Science  
and Instrumentation

Ronald Francis

Accepted.....  
Coordinator, Graduate Program

School of Photographic Arts and Sciences  
Rochester Institute of Technology  
Rochester, New York

CERTIFICATE OF APPROVAL

---

MASTER'S THESIS

---

The Master's Thesis of Mitchell D. Feather  
has been examined and approved  
by the thesis committee as satisfactory  
for the thesis requirement for the  
Master of Science degree

Burt H. Carroll

.....  
RDr. Burt H. Carroll, Thesis Advisor

William S. Shoemaker

.....  
Professor William Shoemaker

Jack Hamilton

.....  
Mr. Jack Hamilton, Eastman Kodak Co.

..... May 23, 1980 .....

THE EFFECTS OF  
CONCURRENT PHOTON AMPLIFICATION  
UTILIZING AN INFRARED LATENSIFICATION SOURCE

by

Mitchell D. Feather

Submitted to the Photographic Science and  
Instrumentation Division in partial fulfillment  
of the requirements for the Master of Science  
degree at the Rochester Institute of Technology

ABSTRACT

An investigation was conducted regarding the effects of varying supplementary exposure on High-Speed Infrared Film. In addition, CPA was evaluated in comparison to Hypersensitization and Latensification. The results were that CPA is superadditive with respect to both density and exposure, the maximum effect being noted in the toe of the characteristic curve. Furthermore, Hypersensitization and Latensification, with dark intervals up to five seconds, displayed efficiency that was not significantly different from CPA. It was also determined that the spectral distribution of the imaging source does not affect the efficiency of CPA. Corroboration of C&C Research's speed increase claims was achieved.

While it is not common practice to place a dedication in a Master's Thesis, I feel it is necessary. To two people who constantly provided the encouragement and strength for me to strive and successfully complete my undergraduate and graduate work in this four year period. To my parents, Samuel and Jean Feather, I dedicate this Master's thesis.

## ACKNOWLEDGEMENTS

If the knowledge gained from people in government and industry is a sign of accomplishment, then this thesis can be considered a success from that aspect alone. To all of these people I extend my deepest gratitude:

Mr. Edward C. Scott of RADC for all of his assistance regarding the state of the art of CPA.

Mr. Mike Cutler of Hewlett Packard for graciously supplying me with the Infrared Emitting Diodes

Mr. Rex McHail of Bausch and Lomb for all of his help and encouragement with my background study in photogrammetry

Mr. Gordon P. Brown of Eastman Kodak Company for his assistance regarding the application of CPA to Kodak Infrared products

Mr. John Carson of Rochester Institute of Technology for his great help in designing and constructing the CPA Sensitometer

Dr. Ronald Francis of Rochester Institute of Technology for planting a seed four years ago that blossomed into this Master's Thesis

Dr. Burt Carroll of Rochester Institute of Technology without who's guidance, none of this would be possible

Dr. Ed Granger and Dr. David Sturmer for their efforts on my behalf during calibration of the CPA sensitometer.

and to the Central Intelligence Agency for their graciousness in the financial backing of my thesis.

## TABLE OF CONTENTS

	<u>page</u>
List of Figures.....	v
Introduction.....	1
Experimental	
Sensitometer Design.....	6
Testing Procedure.....	12
Discussion.....	14
Conclusion.....	48
List of References.....	50
Appendix A.....	52
Appendix B.....	55
Appendix C.....	57

## LIST OF FIGURES

1. Cross-sectional layout of the CPA sensitometer p. 7
2. Digital Control Logic Circuit p. 9
- 2a. Xenon Flash Circuit p. 10
3. Relative IC outputs p. 11
4. Degree of superadditivity (L) as a function of  
of imaging exposure at supplementary exposure  
levels corresponding to no measurable density,  
.15 over B+F, and .26 over B+F. p. 15
5. Superadditivity as a function of supplementary  
exposure with imaging exposure at -2.74 Log rel.H  
corresponding to .08 density p. 16
6. Superadditivity as a function of supplementary  
exposure with imaging exposure at -2.26 Log rel.H  
corresponding to .08 density. p. 17
7. Superadditivity as a function of supplementary  
exposure with imaging exposure at -1.92 Log rel.H  
corresponding to .08 density. p. 18
8. Superadditivity as a function of supplementary  
exposure with imaging exposure at -1.70 Log rel.H  
corresponding to .092 density. p. 19
9. Superadditivity as a function of supplementary  
exposure with imaging exposure at -1.39 Log rel.H  
corresponding to .15 density. p. 20
10. Superadditivity as a function of supplementary  
exposure with imaging exposure at -0.95 Log rel.H  
corresponding to .50 density. p. 21
11. Superadditivity as a function of supplementary  
exposure with imaging exposure at -0.82 Log rel.H  
corresponding to .685 density. p. 22
12. Superadditivity as a function of supplementary  
exposure with imaging exposure at -0.53 Log rel.H  
corresponding to 1.26 p. 23



## LIST OF FIGURES

13. Density as a function of exposure with supplementary exposure corresponding to .15 over over B+F. p. 25
14. Density as a function of exposure with supplementary exposure -1.92 Log rel.H corresponding to no measurable density. p. 26
15. Density as a function of exposure with supplementary exposure -1.45 Log rel.H corresponding to .05 over B+F. p. 27
16. Density as a function of exposure with supplementary exposure -1.31 Log rel.H corresponding to .11 over B+F. p. 28
17. Density as a function of exposure with supplementary exposure -1.26 Log rel.H corresponding to .15 over B+F. p. 29
18. Density as a function of exposure with supplementary exposure -1.16 Log rel.H corresponding to .20 over B+F. p. 30
19. Density as a function of exposure with supplementary exposure -1.10 Log rel.H corresponding to .26 over B+F. p. 31
20. Superadditivity as a function of Density with supplementary exposure at -1.92 Log rel.H corresponding to no measurable density. p. 32
21. Superadditivity as a function of Density with supplementary exposure at -1.45 Log rel.H corresponding to .05 over B+F. p. 33
22. Superadditivity as a function of Density with supplementary exposure at -1.31 Log rel.H corresponding to .11 over B+F. p. 34
23. Superadditivity as a function of Density with supplementary exposure at -1.26 Log rel.H corresponding to .15 over B+F. p. 35
24. Superadditivity as a function of Density with supplementary exposure at -1.16 Log rel.H corresponding to .20 over B+F. p. 36

## LIST OF FIGURES

25. Superadditivity as a function of Density with  $s_{10}$  supplementary exposure at  $-1.1 \text{ Log rel.H}$  corresponding to a  $\#26$  over B+F. p. 37
26. Density as a function of exposure. Imaging exposure made through a Kodak Wratten 121 filter. p. 40
27. Density as a function of exposure. Imaging exposure made through a Kodak Wratten 89B filter. p. 41
28. Superadditivity as a function of dark interval. Imaging exposure at  $-0.53 \text{ Log rel.H}$  p. 43
29. Superadditivity as a function of dark interval. Imaging exposure at  $-0.82 \text{ Log rel.H}$  p. 43
30. Superadditivity as a function of dark interval. Imaging exposure at  $-0.95 \text{ Log rel.H}$  p. 44
31. Superadditivity as a function of dark interval. Imaging exposure at  $-1.39 \text{ Log rel.H}$  p. 44
32. Superadditivity as a function of dark interval. Imaging exposure at  $-1.70 \text{ Log rel.H}$  p. 45
33. Superadditivity as a function of dark interval. Imaging exposure at  $-1.92 \text{ Log rel.H}$  p. 45
34. Superadditivity as a function of dark interval. Imaging exposure at  $-2.26 \text{ Log rel.H}$  p. 46
35. Superadditivity as a function of dark interval. Imaging exposure at  $-2.74 \text{ Log rel.H}$  p. 46
36. Relative Intensity versus Wavelength of  $\text{HEMT-6000 IRED}$  p. 54

## INTRODUCTION

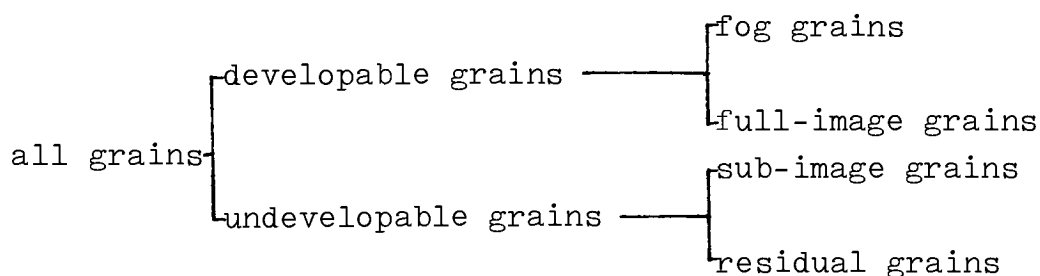
Ever since photography's inchoation, there has been a demand for higher speeds in photographic materials. Various means have been used to achieve these higher speeds, often at the expense of increased grain size, decreased resolution, and other image degradations. One relatively new technique is the use of simultaneous supplementary diffuse exposure, also known as Concurrent Photon Amplification (hereafter, referred to as CPA). With this technique, C&C Research, Inc. has reported speed gains in Black and White films of two to six times without loss of image quality or resolution. Similar results were reported with color reversal materials with speed gains ranging from ten times with good color saturation and resolution, to more than 100 times with some loss of saturation and maximum resolution.<sup>1</sup>

The principles of CPA are based upon a technique whereby non-image radiation is added simultaneously to that of the imaging exposure. Many photographic materials have been used: Black and White, Color Negative, and Color Reversal. The spectral sensitivities have ranged from the visible portion of the spectrum to the Infrared. In every case, the latensification sources possessed spectral distributions mainly in the visible of the spectrum.

The USAF Avionics Laboratory at Wright-Patterson AFB has reported successful results utilizing a near-Infrared latensification source.<sup>2</sup> Due to dimensional characteristics of the camera equipment, the latensification source was placed on the optical axis just in front of the lens.

Prior to considering the mechanism of CPA, it is necessary to review the mechanism of latent image formation with particular attention being paid to the concepts of Reciprocity failure.

Burton & Berg divide all grains into two categories - developable and undevelopable grains.<sup>3</sup> These are subdivided into four categories, as illustrated:



Where fog grains are developable even when no exposure is given and the residual grains are left unaffected by exposure.

The residual grains can result from either no exposure incident on the grain or the formation of a single silver atom. If this center fails to trap a free electron and capture a

second mobile ion, a recombination takes place.

Capture of this silver ion results in a two-atom silver center, completing what they refer to as the nucleation stage. For all practical purposes, this two-atom silver center can be considered stable, but it is still undevelopable. This is what Burton & Berg refer to as the sub-image grain.

This electron-trapping--silver ion capture series of events continues in what they termed the grain growth stage. At some silver aggregate size, the grain becomes developable (full-image grain).

While supporting the Gurney-Mott principle that the latent-image formation process consists of electronic and ionic stages, the work of Burton & Berg has indicated that the inefficiencies are not the same for both stages of formation of the latent-image center. They demonstrated that the nucleation stage (formation of stable sub-speck) is efficient with High Intensity exposure, while inefficient at Low Intensity. Furthermore, it was also shown that the growth stage (Building up of stable sub-speck to developable size) is efficient at Low Intensity while inefficient at High Intensity.

Relative to this thesis, the most significant result of

Burton's and Berg's work<sup>4</sup> is that a low intensity post exposure acts efficiently in grains bearing stable sub-specks, inefficiently in residual grains, resulting in revelation of the sub-image. A further conclusion of this work, Webb & Evans<sup>5</sup>, Hartree & Hill<sup>6</sup>, and Alter, Barber, & Edwards<sup>7</sup> was that the combination of high and low intensity exposures is more effective if the high intensity portion comes first.

Since it has already been determined by Burton & Berg that the developed density due to the successive application of imaging and supplementary exposures is greater than the sum of the densities produced by the same exposures when applied separately,<sup>8</sup> it is the intent of this work to determine the magnitude of this "superadditive" effect in the case of concurrent application of the imaging and supplementary exposures. It is at this point that the hypothesis is presented that this superadditive effect will be of greater magnitude than in the case of successive application of HI-LI exposures. It is felt that there will be no greater efficiency in revealing the sub-image and that sub-speck formation at very low intensity is a chance process. However, it has been determined by Burton & Berg that a Low Intensity exposure can act upon the speck in the nucleation stage and build the speck up to developable size. It is those full specks that would account for the difference between concurrent and successive supplementary exposures.<sup>9</sup>

Since this "superadditivity" resulting from the application of a supplementary exposure is physically equivalent to reducing the magnitude of the imaging exposure necessary to produce a given image density, thus resulting in an apparent increase in speed, it can be determined whether a supplementary diffuse infrared exposure will produce the type of speed increases stated by C&C Research.

The importance of these objectives lies relative to a key potential application of Infrared CPA, Infrared Aerial Photography.

In Infrared Aerial Photography, there currently exists a significant trade-off between resolution and film speed. The net result of this trade-off is that the use of High Definition Aerial Infrared materials demands a sacrifice of slower camera speeds and/or higher flying altitudes.

Since it has previously been determined that CPA has no adverse effects on Image quality, CPA seems like a logical solution to bringing High Definition Aerial Materials up to a working speed equivalent to the higher speed materials. The ultimate intent here is to determine if CPA can provide a sufficient increase in speed to do this, since both pre-exposure and post-exposure by the supplementary source would be undesirable since both techniques would complicate timing sequences during mapping and reconnaissance missions.

## EXPERIMENTAL

### Sensitometer Design

In order to properly examine CPA with respect to what Burton and Berg refer to as hypersensitization and latent-image intensification<sup>10</sup> (which respectively refer to the techniques where a supplementary pre-exposure hypersensitizes the material to the imaging exposure and a supplementary post-exposure intensifies the latent image produced by the previous imaging exposure), the variable factors considered were supplementary exposure intensity and time difference between initiation of imaging and supplementary exposures ( $\Delta t$ ). The factors of supplementary exposure time, imaging exposure time and intensity, and length of time between imaging exposure and development were all kept fixed.

In order to supply the quantitative data required for this evaluation, it was necessary to construct an intensity-scale sensitometer which allowed for changes in the intensity of the supplementary source. In addition,  $\Delta t$  had to change from latensification to hypersensitization, including CPA. Furthermore, the supplementary exposure could not be modulated by the test target (step tablet). It was felt that the best approach to meeting these requirements was in-camera sensitometry.

From an optical aspect, the sensitometer consists of a Xenon



flash diffusely illuminating a test target which is imaged on the film plane of a Canon Ftbm 35mm SLR. The Xenon flash circuit is based upon the original circuit designed for the EG&G Mark VI flash sensitometer. Hewlett-Packard HEMT-6000 Infrared Emitting Diodes (hereafter referred to as IRED's) were chosen as the supplementary exposure source to be mounted in the camera. The diode characteristics appear in the Appendix. After installing the IRED's and aiming them by visual judgement, a diffusant was applied to the IRED's in order to reduce their specular characteristics. Kodak film type High Speed Infrared was utilized as a detector in fine adjustment of trimmer resistors  $R_8$ - $R_{13}$  (see Figure 2). The result of this adjustment was variability of  $\pm 0.003$  density units at a mean density of 0.704 (alpha risk of 0.05), thus providing a diffuse supplementary exposure source.

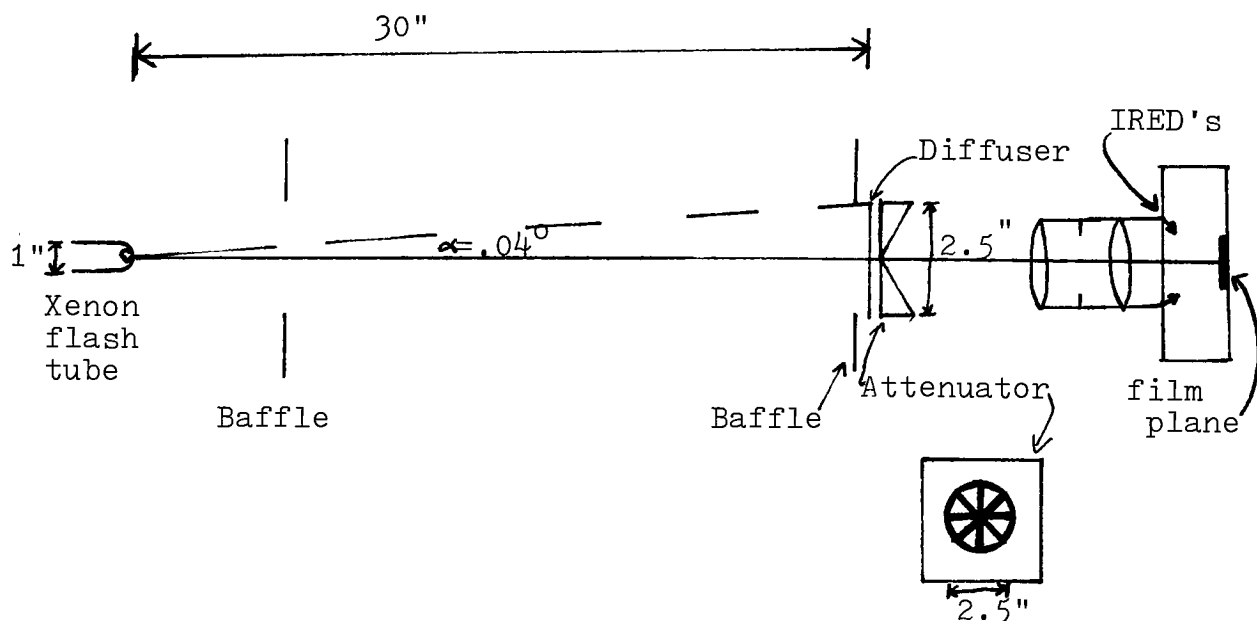


Fig. 1. Cross-sectional layout of the CPA sensitometer.

The attenuator is of circular construction, fabricated from flashed film. The film used was Kodak film type Fine Grain Positive. The eight step circular design was chosen to minimize any variations in intensity (based upon the Cosine Law) uniform for all steps. Based upon the Cosine<sup>4</sup> Law, the minimum off-axis radiance was calculated to be 99.9999% of the on-axis radiance. The sensitometer is lined and baffled to minimize stray light.

The heart of the CPA sensitometer is the Digital Control Logic Circuitry, which has four basic functions:

- control IRED intensity
- control IRED exposure
- trigger Xenon flash
- control time delay between Xenon and IRED exposures

As Figure 2 indicates, the circuitry is based upon 555 IC timers with a Double Pole Double Throw switch ( $S_2$ ) allowing for both hypersensitization and latensification.

Upon application of the five volt triggering pulse, by means of  $S_1$ , the output (pin 3) of  $IC_1$  goes to a logic state of 1. After a time interval determined by the  $R_1C_1$  network, the output returns to 0-state. The  $R_2C_3$  network prevents any possibility of mistriggering on positive edges (as does  $R_4C_6$  and  $R_6$ ). Switch 2 determines whether this output drives the

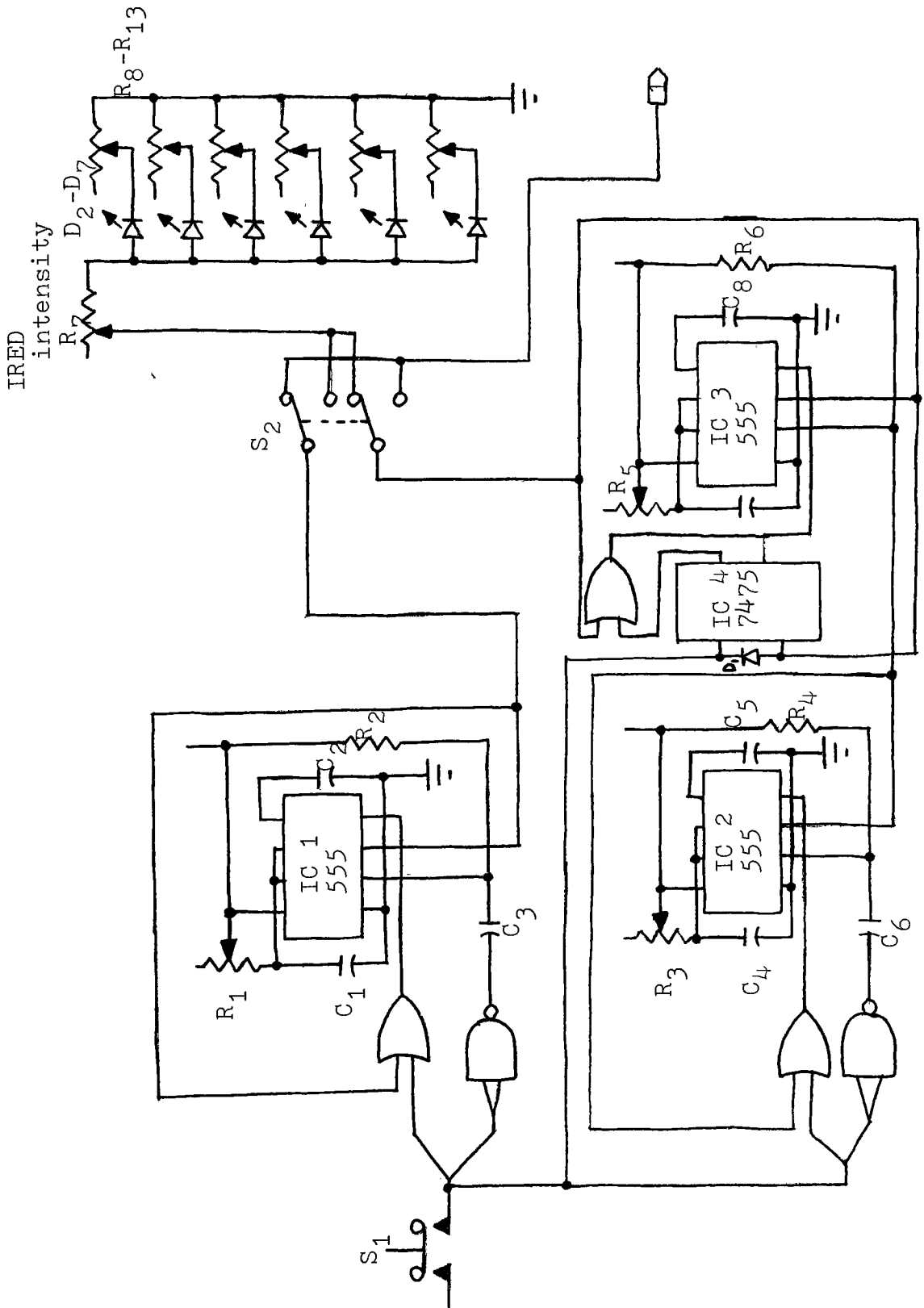


Fig. 2. Digital Control Logic Circuit

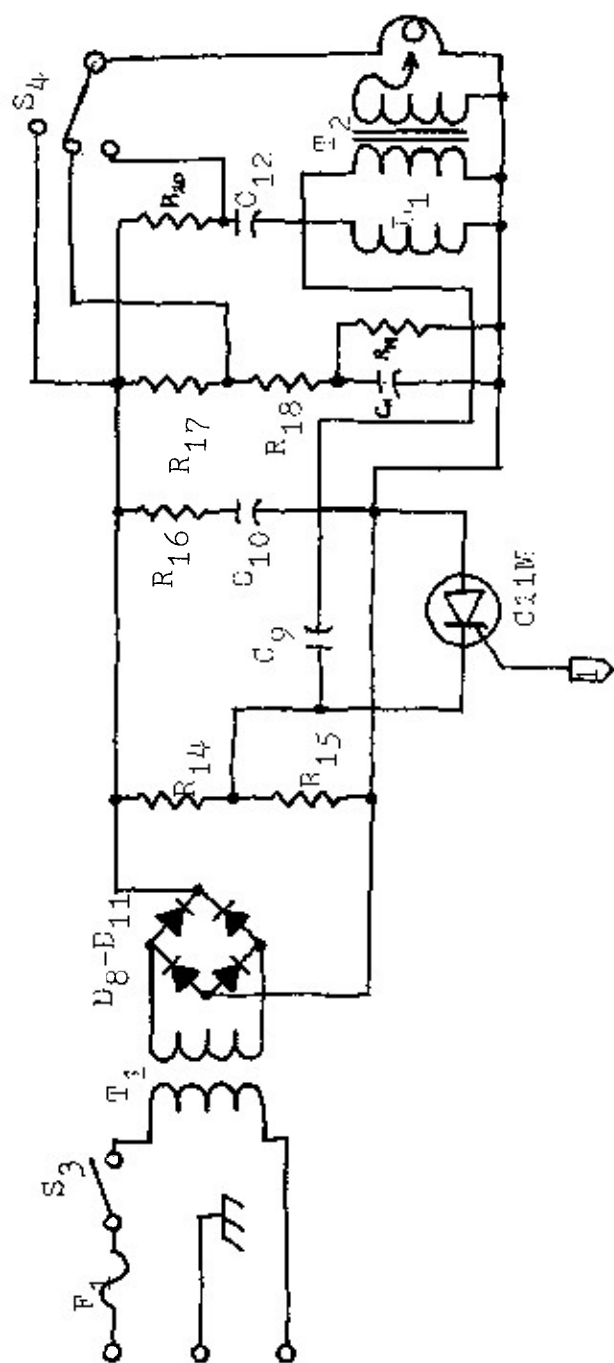


Fig. 2a. Xenon Flash Circuit

IRED's or triggers the Xenon Flash.

Concurrent with the triggering of  $IC_1$ , is the triggering of  $IC_2$ . Once again, the  $R_3C_4$  network regulates the output pulse width, thus regulating the time delay between exposures. An infinitesimal period ( $\sim 10^{-4}$  seconds) after the application of  $V+$  at  $S_1$ , the output of  $IC_4$ , a bistable latch, goes to a 1-state. The output of  $IC_4$  doesn't return to a 0-state until the output of  $IC_3$  changes to the 1-state. Pin 4 of  $IC_3$  stays high until the output of  $IC_3$  goes low, by means of an OR gate. With pin 4 in a 0-state,  $IC_3$  would be disabled. The prevention of false triggering of  $IC_3$  summarizes the function of the bistable latch. Figure 3 illustrates the various IC outputs, with  $t_0$  representing the application of a triggering pulse at  $S_1$ .

Supplementary exposure intensity is controlled by a variable resistor ( $R_7$ ) in series with all of the IRED's. As indicated in Figure 2a, the five volt logic circuit triggers the Xenon flash circuit by means of a Silicon Controlled Rectifier (SCR).

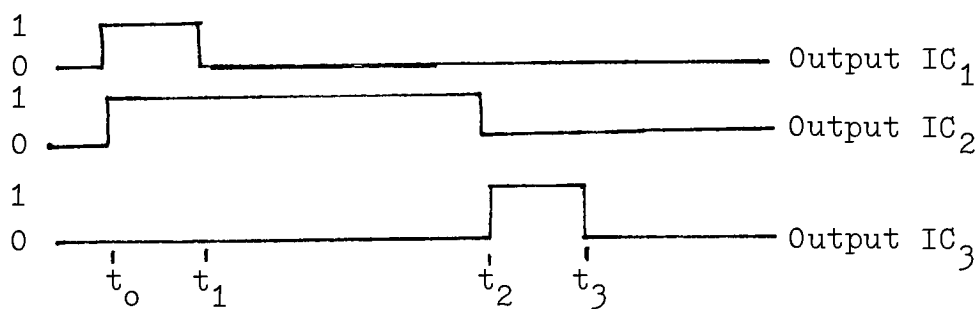


Fig 3. Relative IC outputs

### Testing Procedure

As a means of avoiding any variability between rolls of film, the response variable considered was the developed density due to application of both imaging and supplementary exposures to the same region in comparison to the densities produced by the same exposures when applied separately. In the case of separate exposures, the densities considered are net densities, that is, density above Base + Fog of an unexposed area. As per Burton's and Berg's model, the Density due to double exposure ( $D_{12}$ ) can be represented as:

$$D_{12} = f + D_1 + D_2 + L$$

where  $f$  represents Base + Fog,  $D_2$  is the net density resulting from the supplementary exposure,  $D_1$  is the net density resulting from the Imaging exposure, and  $L$ , the amount of superadditive density, may be positive or negative.<sup>11</sup> It is this quantity,  $L$ , that was monitored throughout the testing and analysis. Furthermore, an investigation was made to determine whether CPA is superadditive in terms of exposure (viz. superadditivity being indicated by the CPA characteristic curve lying to the left of the additive model.).

The initial phase of testing consisted of adjusting the IRED intensity until  $L$  was maximized for the case of both exposures being concurrent.

Once the system was optimized, the CPA technique was examined

relative to hypersensitization and latensification, by means of L. For this part of the study,  $\Delta t$  ranged from -30 seconds(hypersensitization) to +30 seconds(latensification).

The final phase of this investigation, the efficiency of CPA was examined with the imaging exposure, (1) unfiltered, (2) filtered by a Kodak Wratten 12 filter, and (3) filtered by a Kodak Wratten 89B filter.

The film chosen for this study was Kodak film type High Speed Infrared,<sup>12</sup> hereafter referred to as HSIR. This choice was based upon this film's similarities to Kodak's Infrared Aerial films in sensitizing dye characteristics.<sup>13</sup>

Processing was in D-19 for six minutes at 68°F, in an agitator similar in design to Dave Porter's agitator<sup>14,15</sup>, which provides continuous tumble activity at thirty tumbles per minute. Relative to processing, Development Uniformity tests were carried out utilizing Kodak Film Type Panatomic-X because of its fine grain characteristics. An 18% gray card was uniformly illuminated(no detectable variations in luminance) and imaged onto the 35mm film. There was no detectable variation in diffuse density across the width of the film and a total variation of 0.017 at a mean density of 1.024. In addition, a Development Lag test was carried out, where the time from exposure to processing varied from three minutes

to twenty-four hours. Utilizing the previous set-up, but with Kodak film type High Speed Infrared, no significant variation in density (at an alpha risk of 0.05) was found due to development lag.



## DISCUSSION

Response to uniform supplementary exposures of varying intensities was determined by experiment. At 0.1 second exposure time, the supplementary exposures ranged from those giving no measurable density when used alone, to 0.26 over Base + Fog. The results of this part are summarized in Figure 4, which represents L, the amount of superadditive density as a function of Log Exposure (imaging exposure) for varying supplementary exposures. These results are superimposed with the Control (no supplementary exposure) characteristic curve as a matter of reference. The results are also examined in Figures 5-12 which represent L as a function of IRED exposure for varying imaging exposures. By inspection, it can be determined that CPA is a superadditive technique in terms of the photographic effect. It can also be seen that this superadditive effect is most pronounced in the region of the characteristic curve where the toe breaks into the straight-line portion. As the shoulder of the characteristic curve is approached, the effect of the supplementary exposure decreases. From these results, a hypothesis is proposed that the highest concentration of stable sub-specks is at that point where the toe of the curve breaks into the straight line portion. This concentration tapers off until Dmax is reached at which point the sub-speck concentration is negligible.

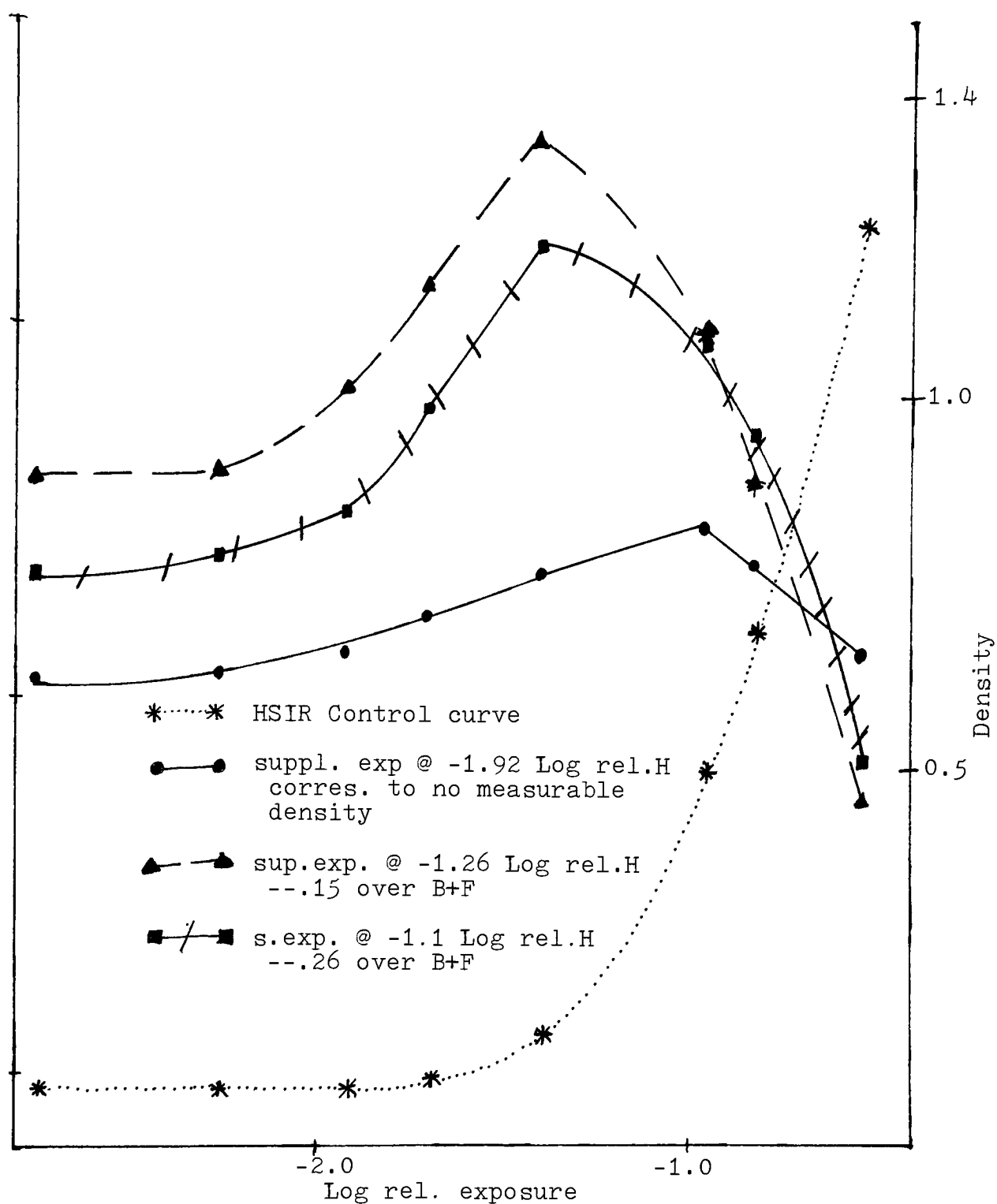


Fig. 4. Degree of superadditivity (L) as a function of imaging exposure at supplementary exposure levels corresponding to no measurable density, .15 over B+F, and .26 over B+F.

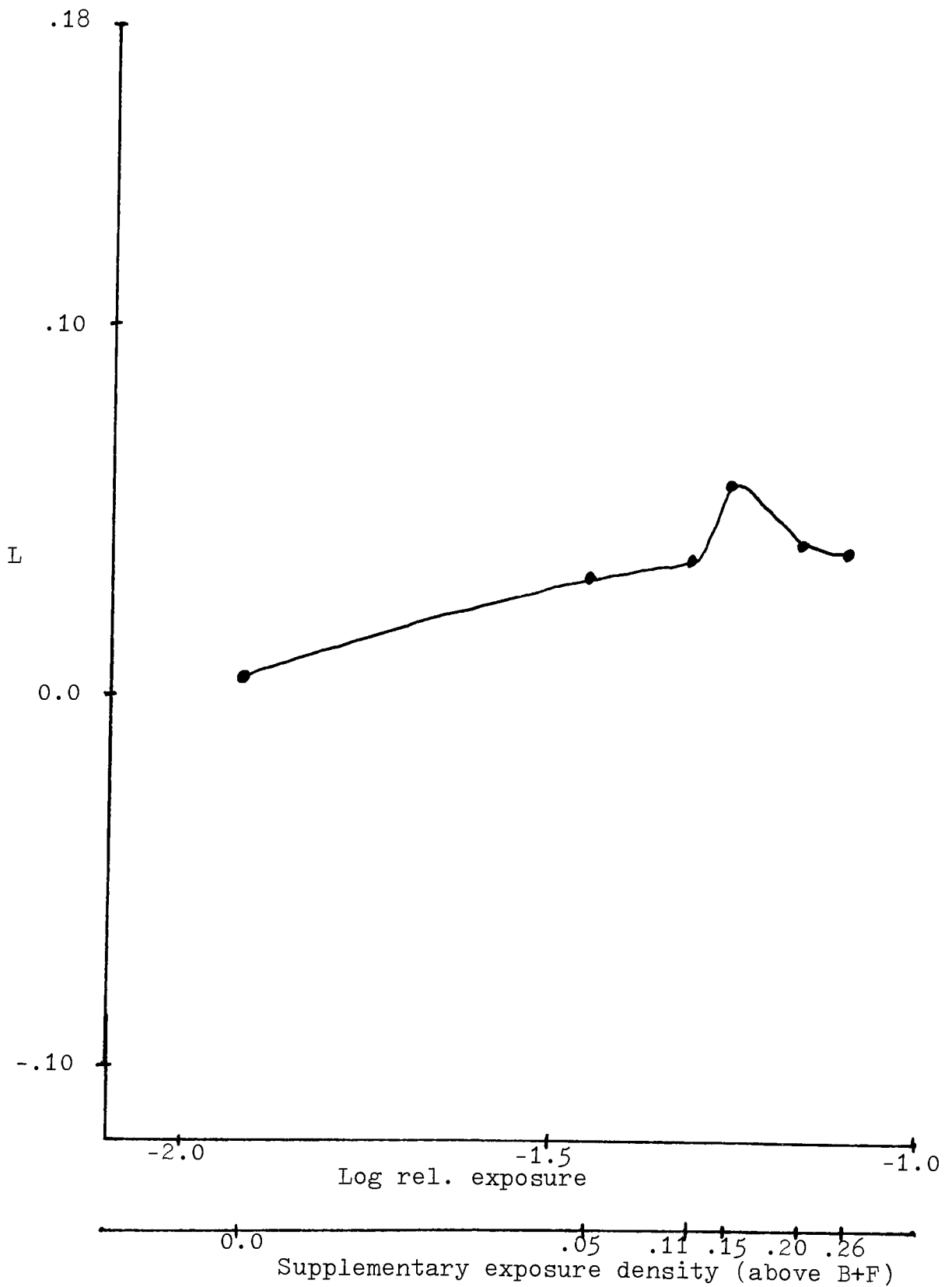


Fig. 5. Superadditivity as a function of supplementary exposure with imaging exposure at  $-2.74$  Log rel.H corresponding to .08 density

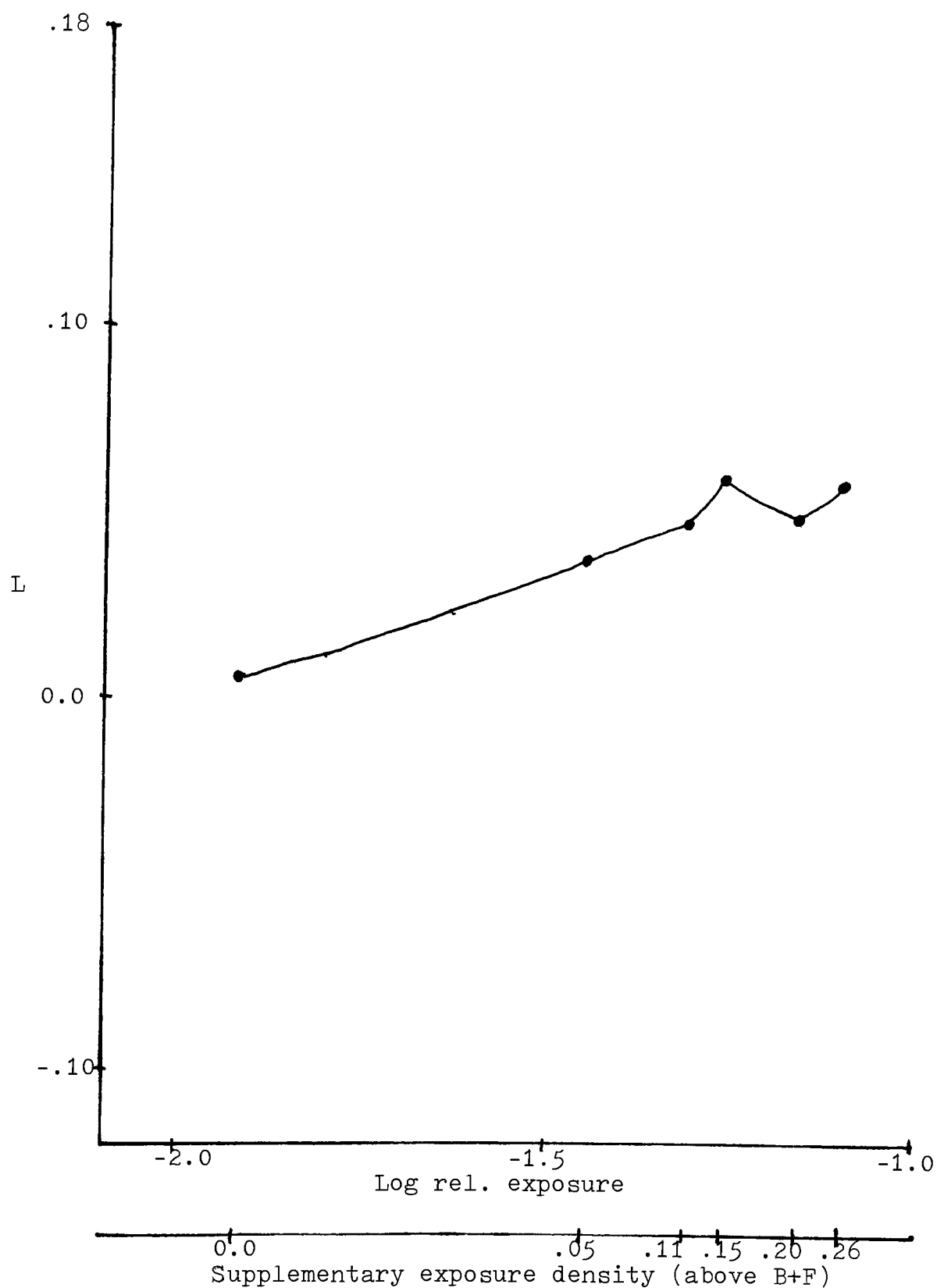


Fig. 6. Superadditivity as a function of supplementary exposure with imaging exposure at -2.26 Log rel.H corresponding to .08 density

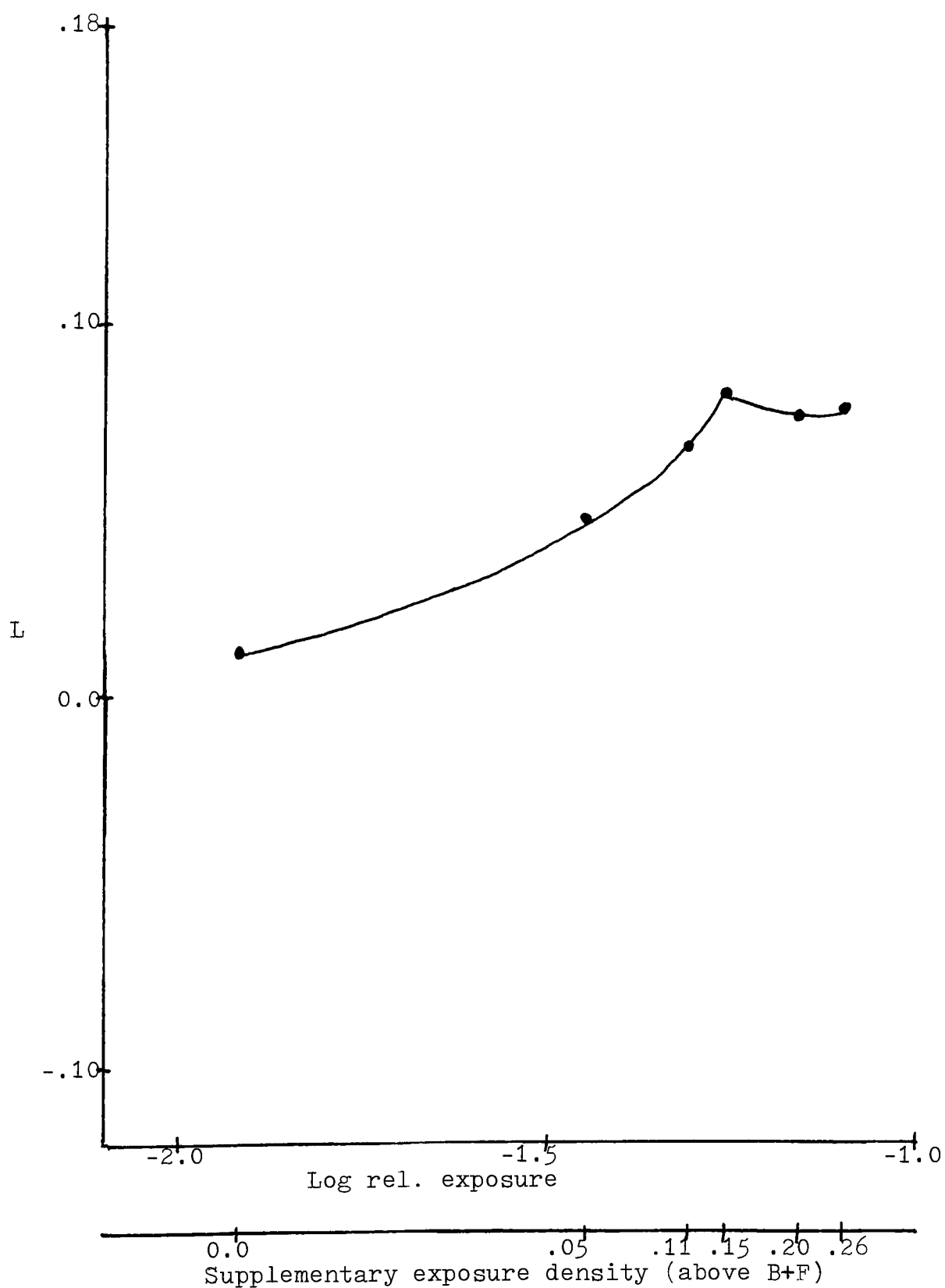


Fig. 7. Superadditivity as a function of supplementary exposure with imaging exposure at  $-1.92$  Log rel.H corresponding to .08 density

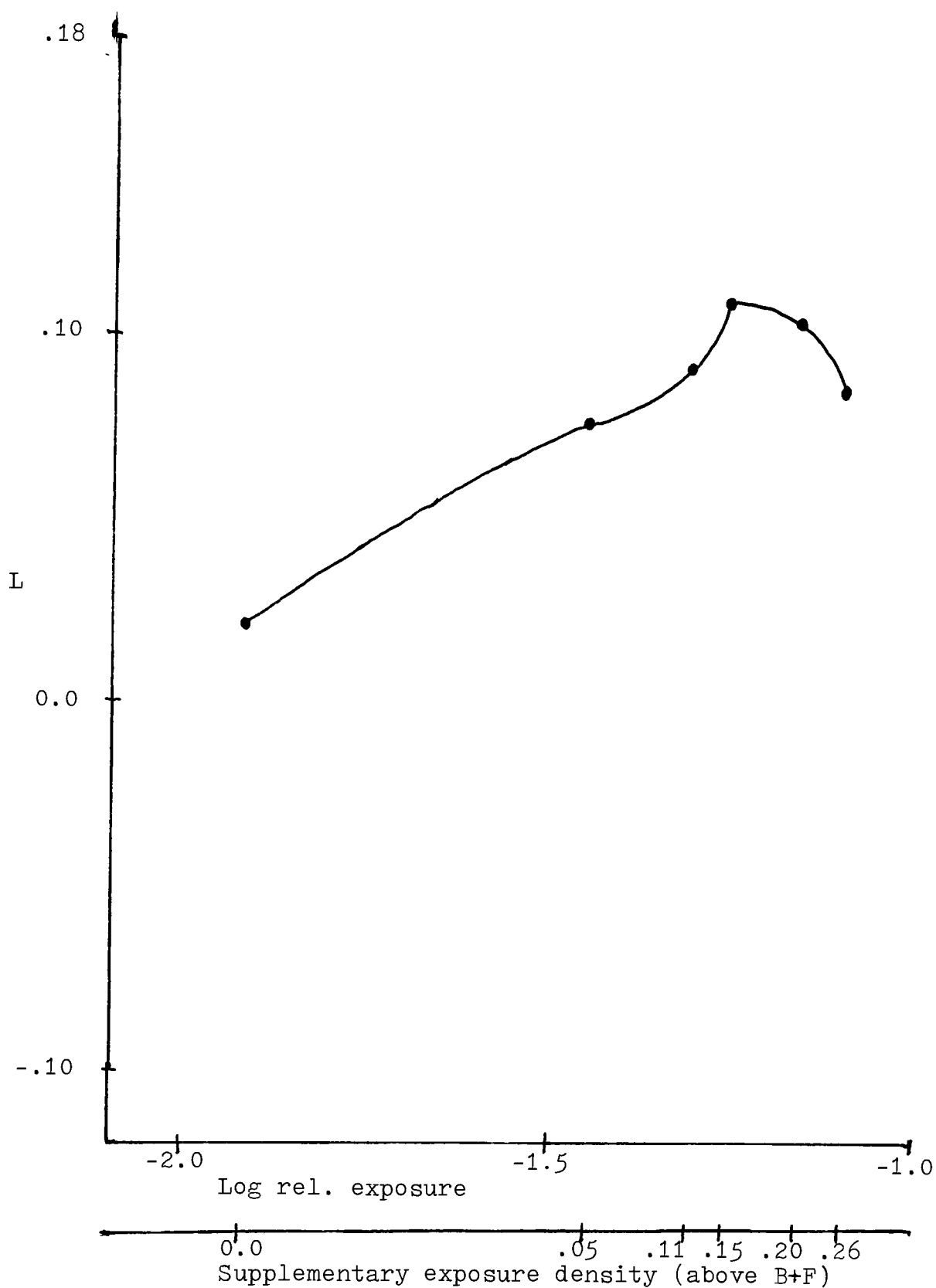


Fig. 8. Superadditivity as a function of supplementary exposure with imaging exposure at  $-1.70$  Log rel.H corresponding to  $.092$  density

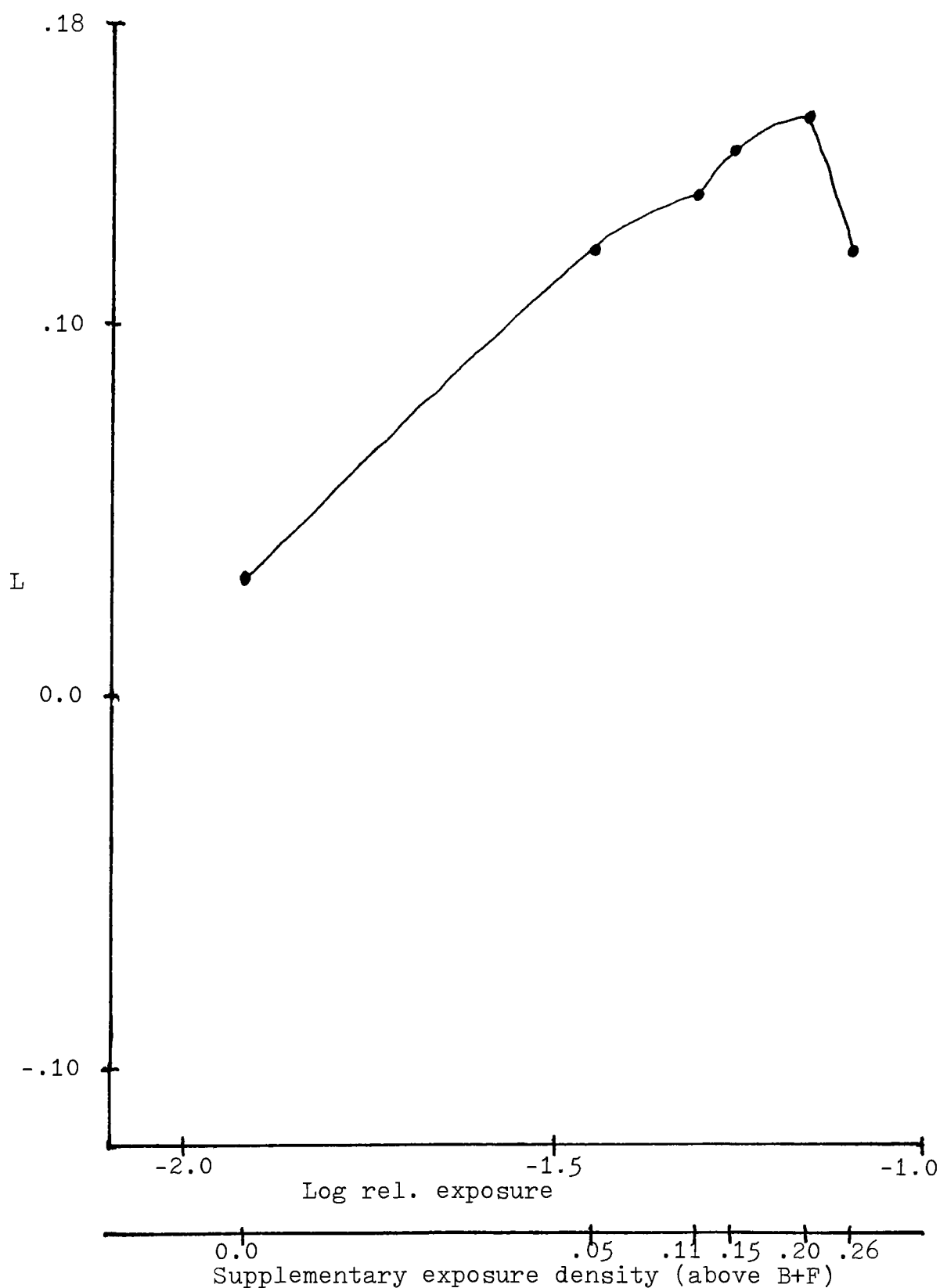


Fig. 9. Superadditivity as a function of supplementary exposure with imaging exposure at  $-1.39$  Log rel.H corresponding to .15 density

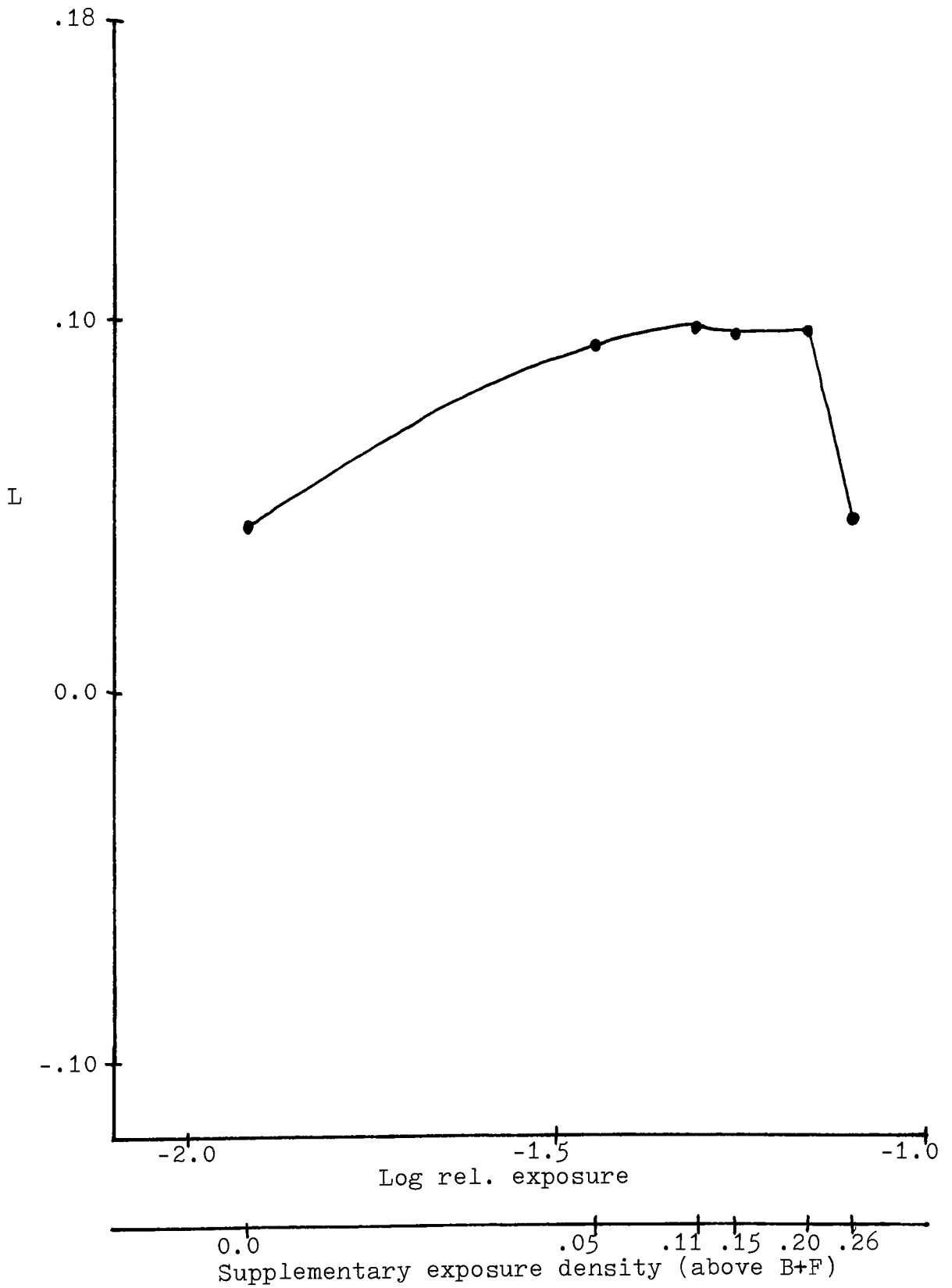


Fig. 10. Superadditivity as a function of supplementary exposure with imaging exposure at  $-0.95$  Log rel.H corresponding to .50 density



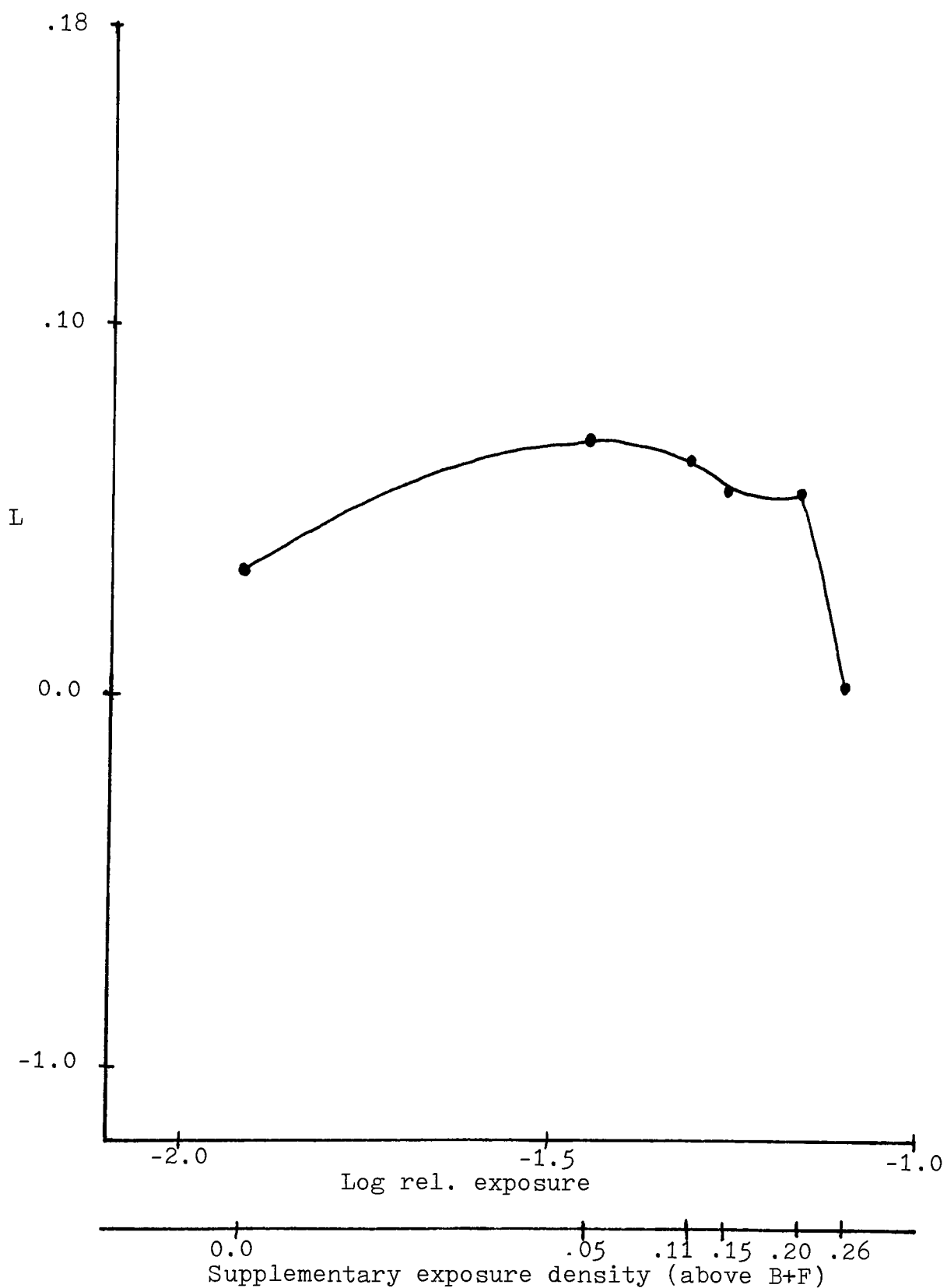


Fig. 11. Superadditivity as a function of supplementary exposure with imaging exposure at  $-0.82$  Log rel.H corresponding to .685 density

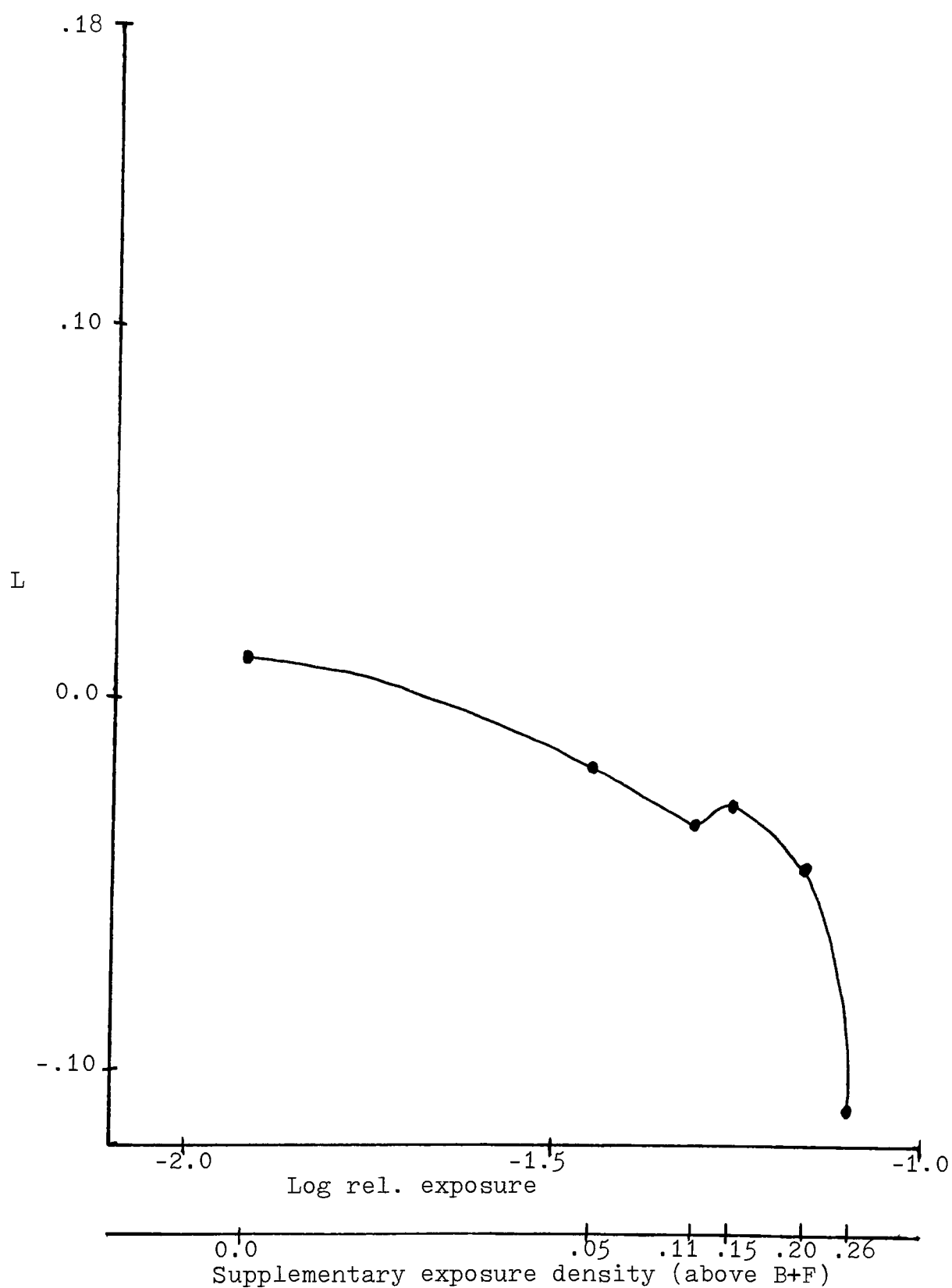


Fig. 12. Superadditivity as a function of supplementary exposure with imaging exposure at  $-0.53$  Log rel.H corresponding to 1.26 density

As a matter of thoroughness, an investigation was carried out to determine if CPA is superadditive in terms of exposure. In order to achieve this it was necessary to generate a model similar in concept to Burton's and Berg's superadditive density model<sup>16</sup>. When density is examined as a function of relative (imaging) exposure, lies to the left of the curve of the imaging exposure alone (control). Of CPA is strictly additive, then it will lie a distance equal to  $H_s$  to the left of the control curve, for a given density. Therefore, an additive model curve can be generated in the form of  $D_i$  versus  $(H_i - H_s)$ , where  $D_i$  is the density corresponding to an imaging exposure,  $H_i$ .  $H_s$  represents the supplementary exposure. An example of the result of this model appears in Figure 13. This model can be extended to the D-Log H format by considering the additive model characteristic curve as  $D_i$  versus  $\log (H_i - H_s)$ . Figures 14 to 19 illustrate the CPA and Control characteristic curves relative to the additive model. At a given density, one can define  $\Delta \log H$  as the separation distance between the Control and CPA curves. If CPA is strictly additive in terms of exposure,  $\Delta \log H$  will equal the separation distance between the Control and additive curves. Based upon this, the model for the double exposure technique is:

$$\Delta \log H_D = \log H_{i_D} - \log (H_i - H_s)_D + S$$

where the subscript D indicates a fixed density,  $\log H_D$  equals  $\log H_{\text{control}} - \log H_{\text{CPA}}$ , and S can be positive or

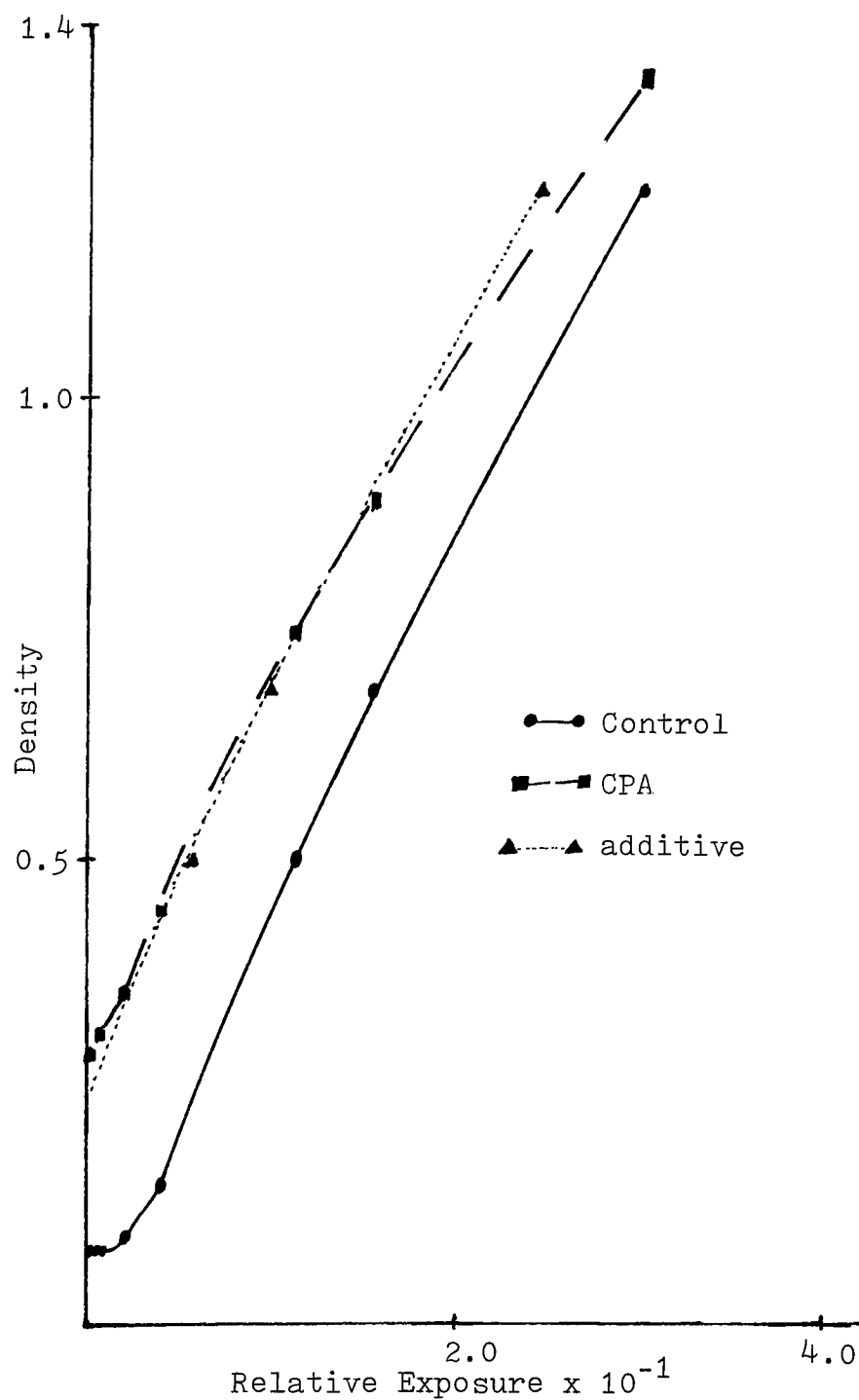


Fig. 13. Density as a function of exposure with supplementary exposure corresponding to .15 over B+F

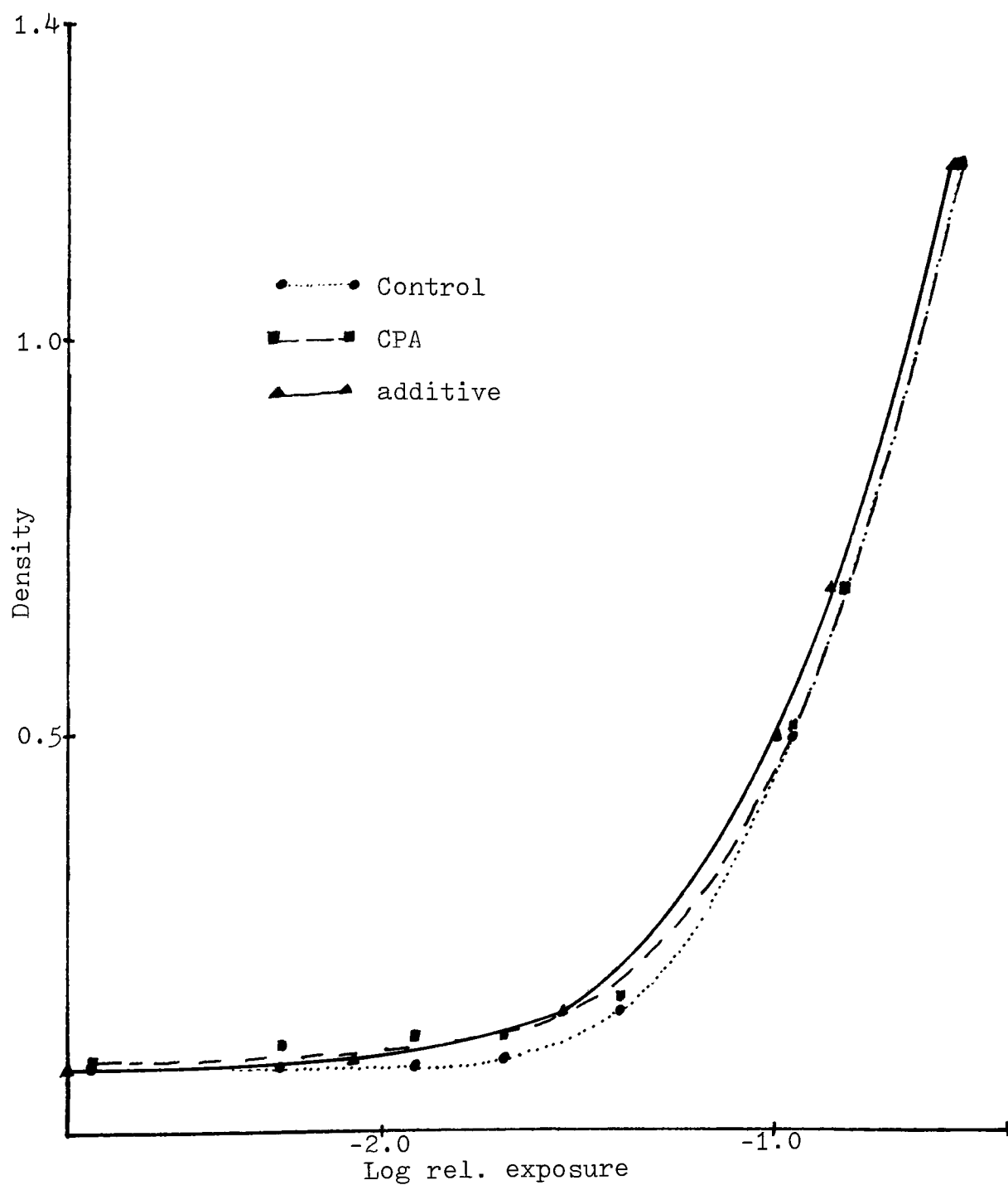


Fig. 14. Density as a function of exposure with supplementary exposure  $-1.92 \text{ Log rel.H}$  corresponding to no measurable density.

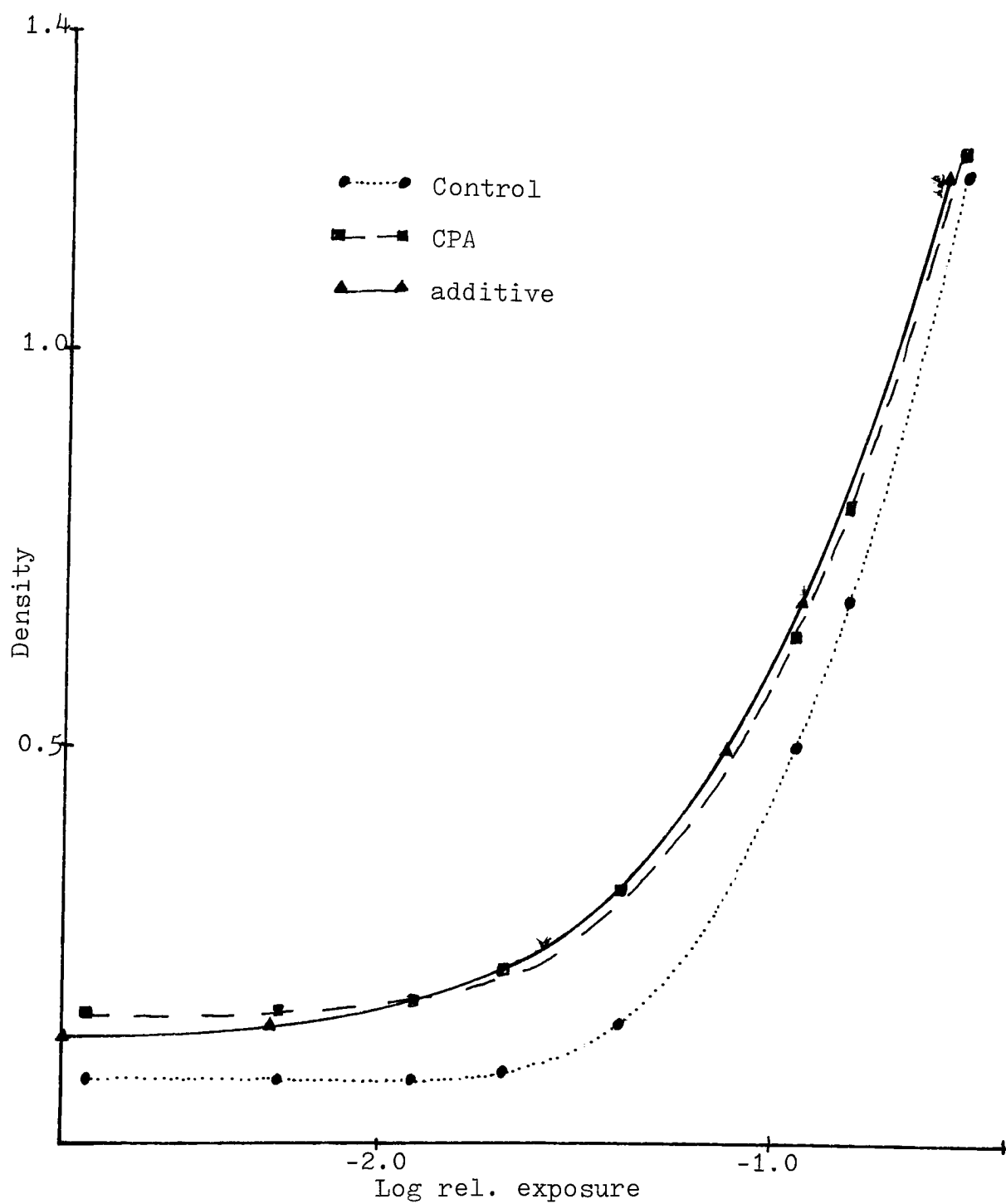


Fig. 15. Density as a function of exposure with supplementary exposure  $-1.45 \text{ Log rel.H}$  corresponding to .05 over B+F.

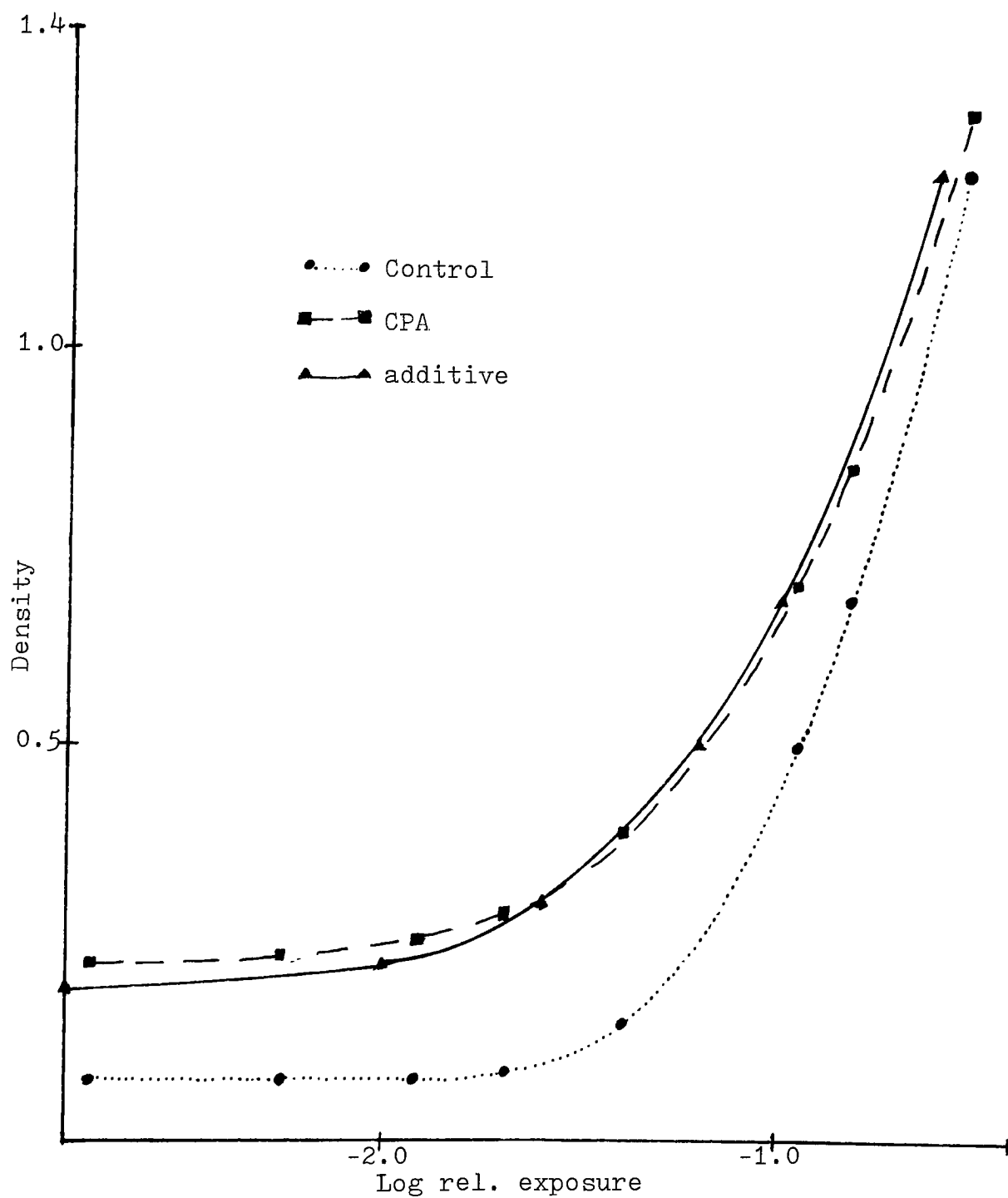


Fig. 16. Density as a function of exposure with supplementary exposure  $-1.31 \text{ Log rel.H}$  corresponding to .11 over B+F

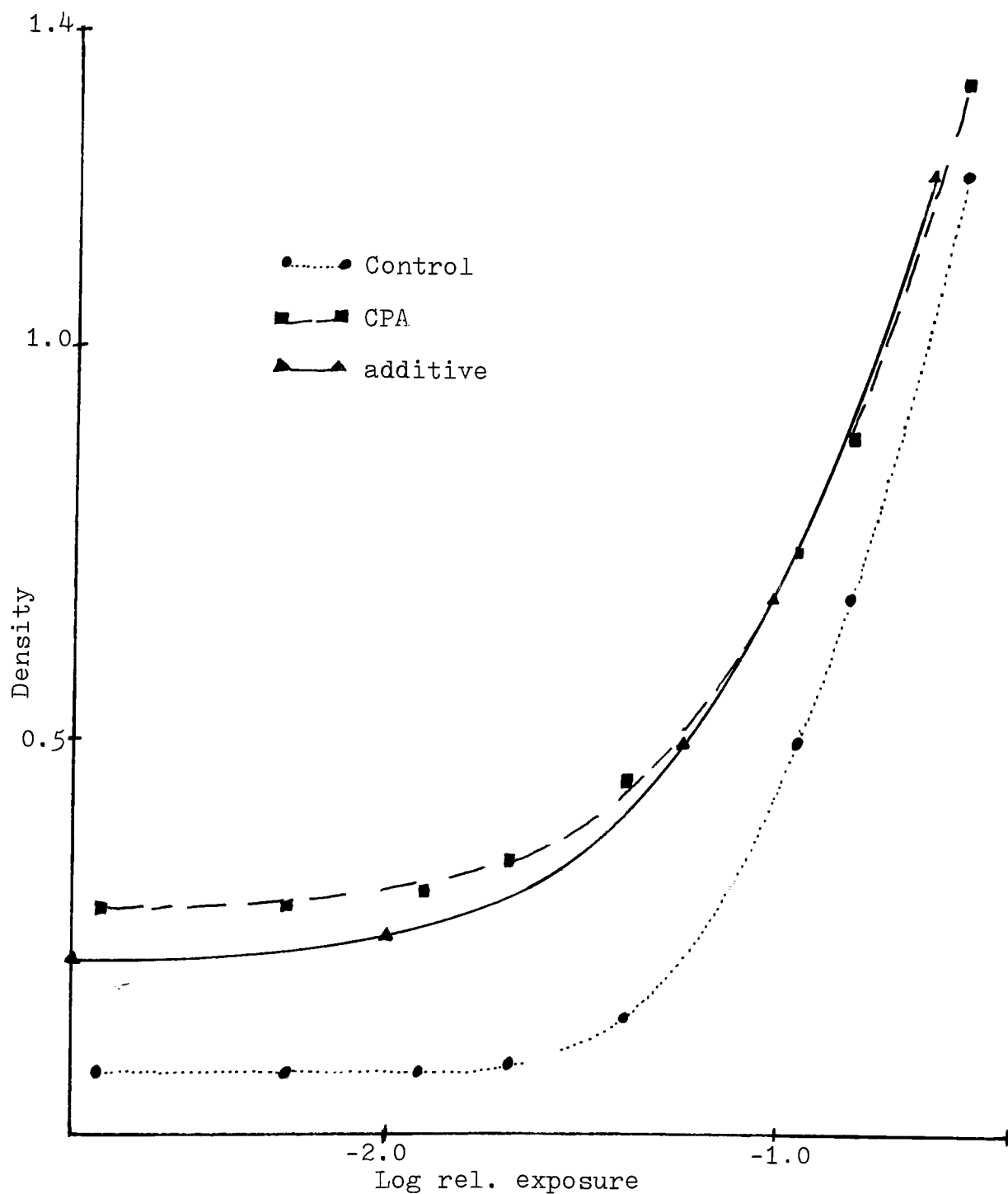


Fig. 17. Density as a function of exposure with supplementary exposure  $-1.26 \text{ Log rel.H}$  corresponding to .15 over B+F



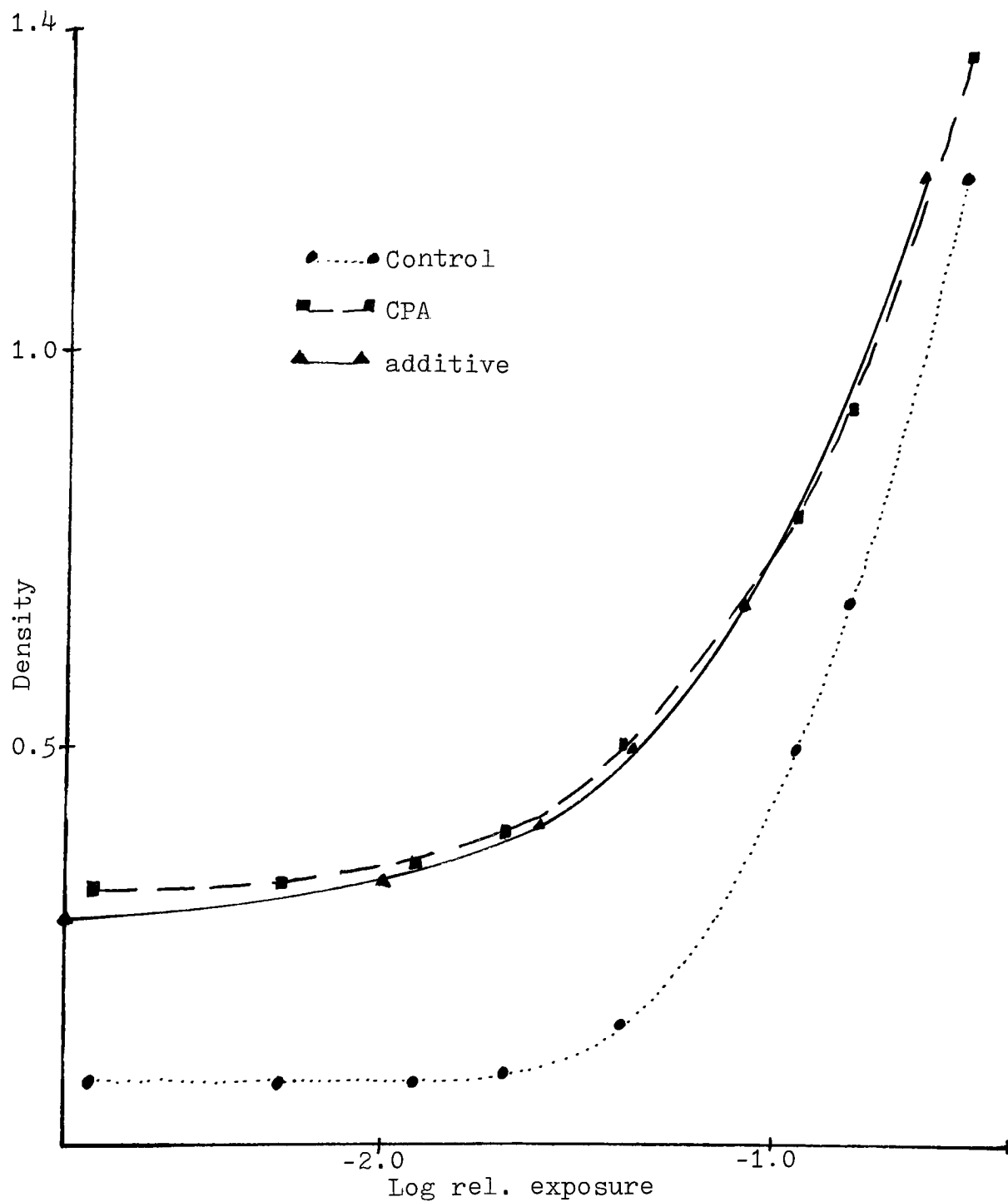


Fig. 18. Density as a function of exposure with supplementary exposure  $-1.16 \text{ Log rel.H}$  corresponding to .20 over B+F

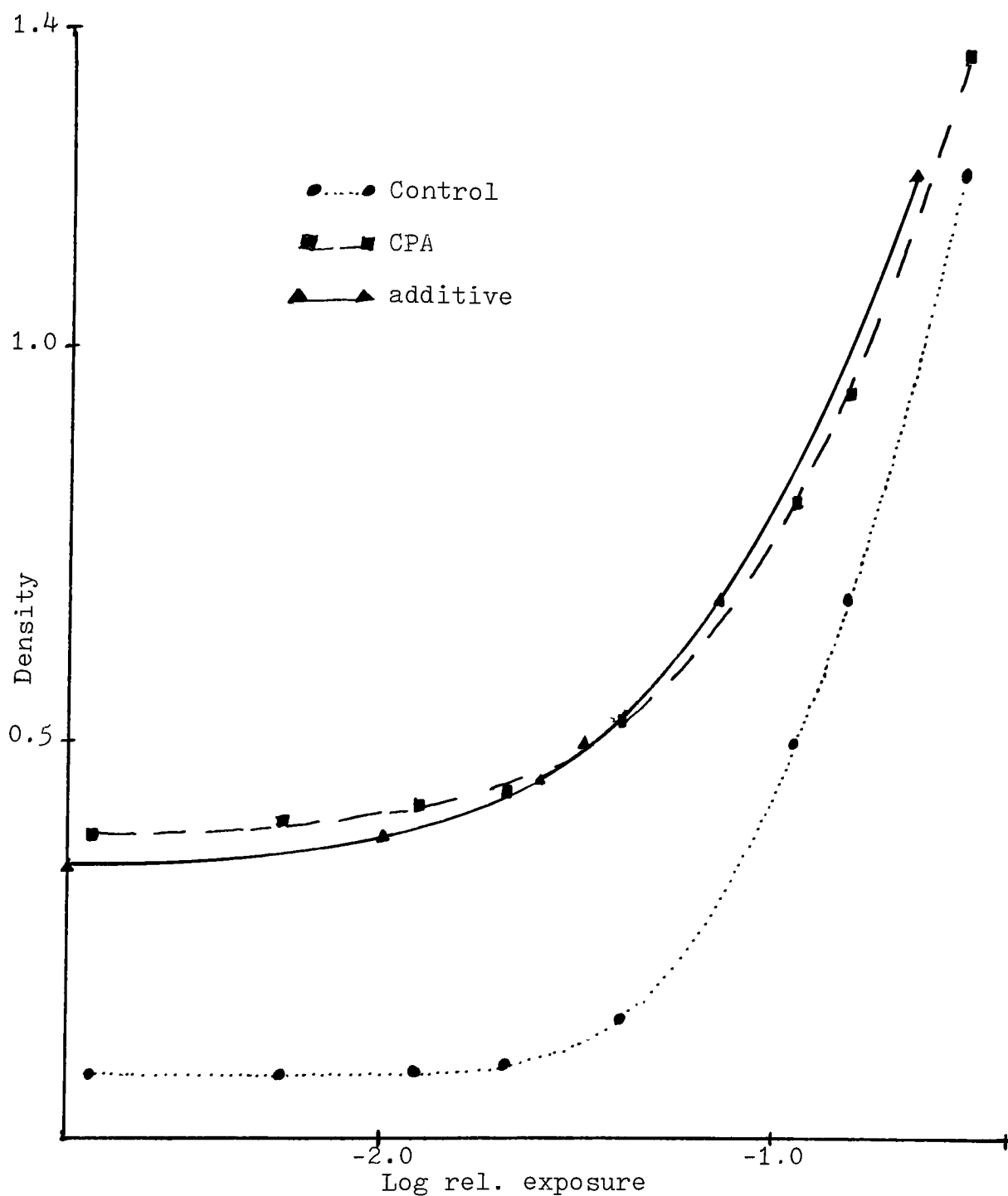


Fig. 19. Density as a function of exposure with supplementary exposure  $-1.10 \text{ Log rel.H}$  corresponding to .26 over B+F

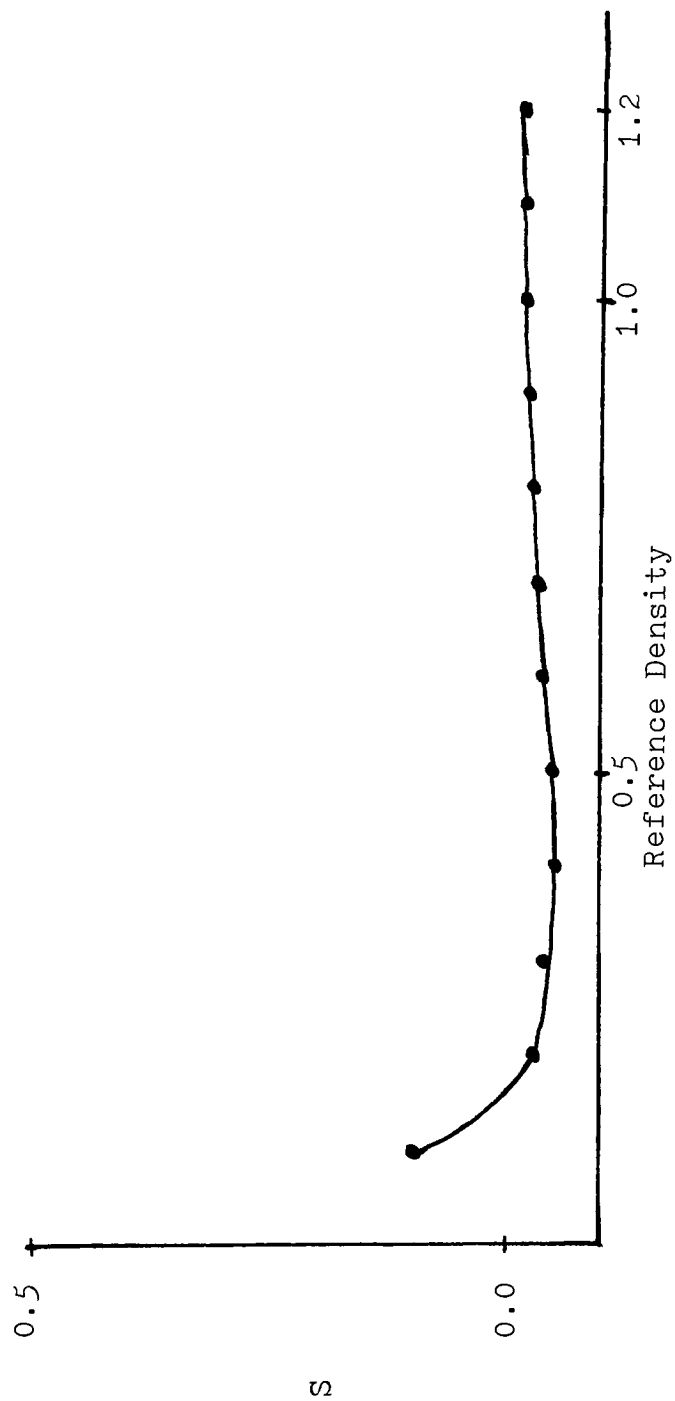


Fig. 20. Superadditivity as a function of Density with supplementary exposure at -1.92 Log rel.H corresponding to no measurable density.

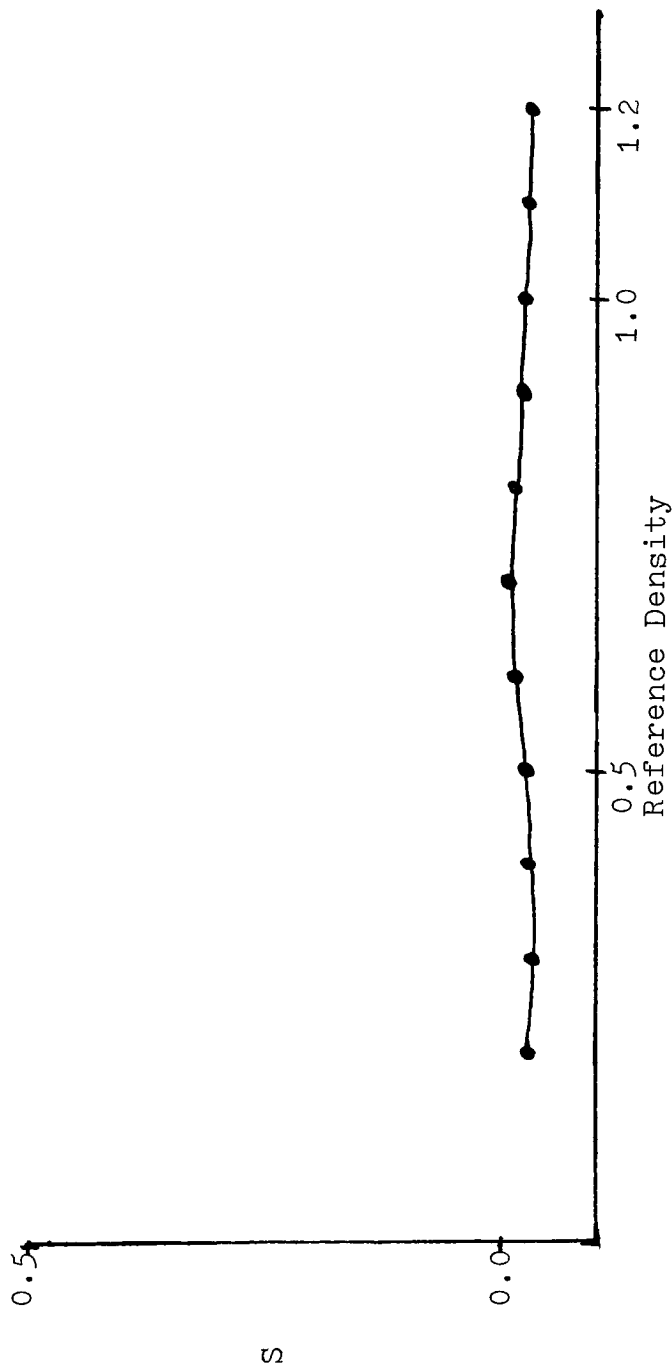


Fig. 21. Superadditivity as a function of Density with supplementary exposure at  $-1.45 \log \text{rel.H}$  corresponding to .05 over  $B+F$

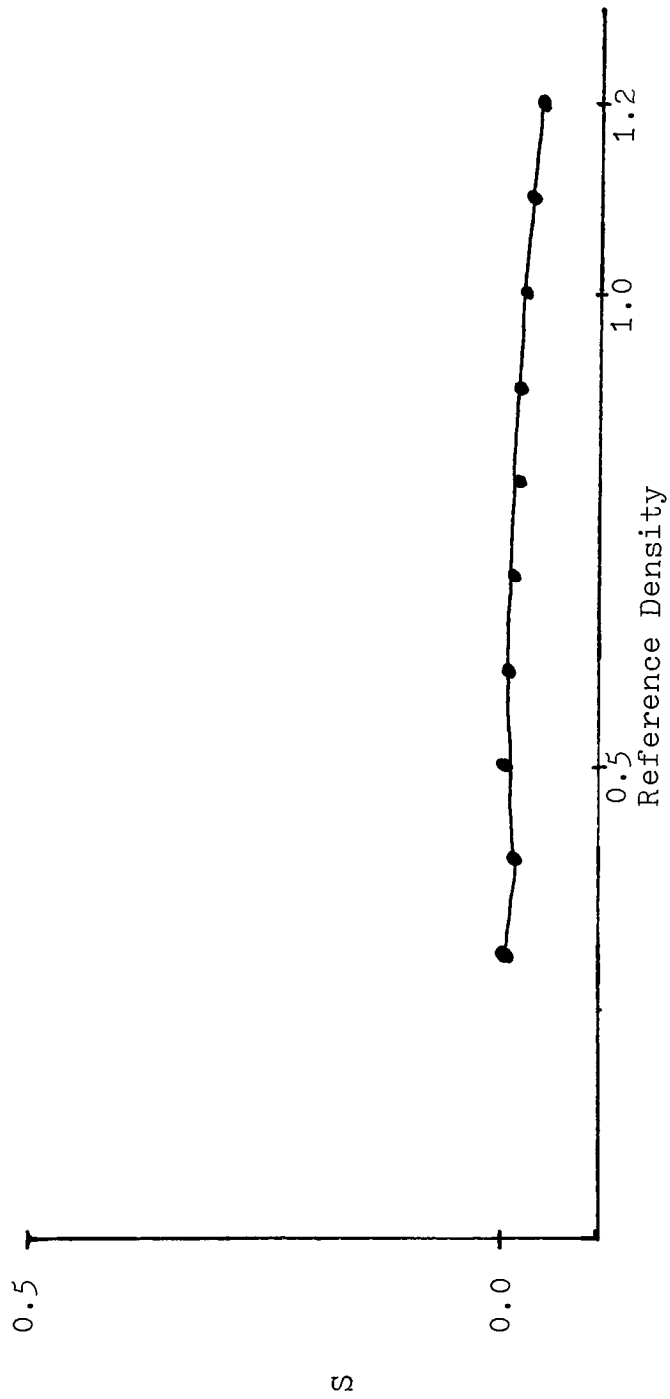


Fig. 22. Superadditivity as a function of Density with supplementary exposure at  $-1.31 \log \text{ rel.H}$  corresponding to .11 over B+F

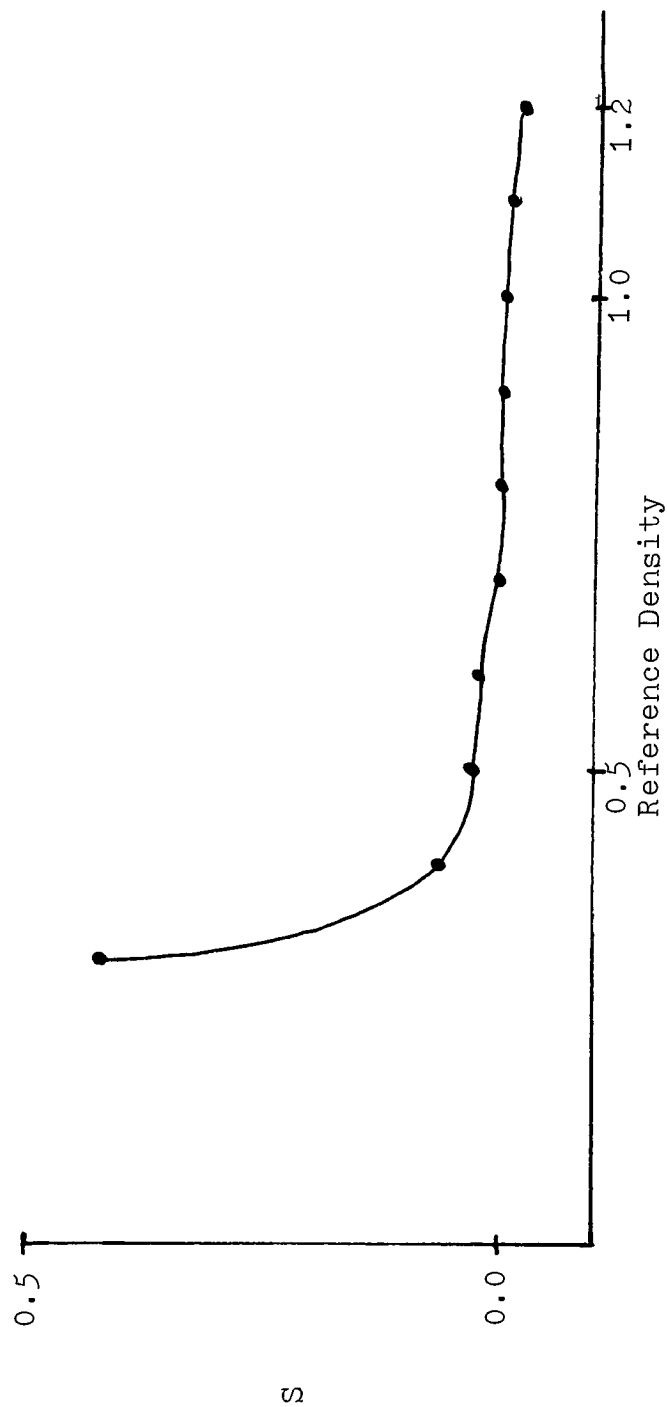


Fig. 23. Superadditivity as a function of Density with supplementary exposure at -1.26 Log rel.H corresponding to .15 over B+F

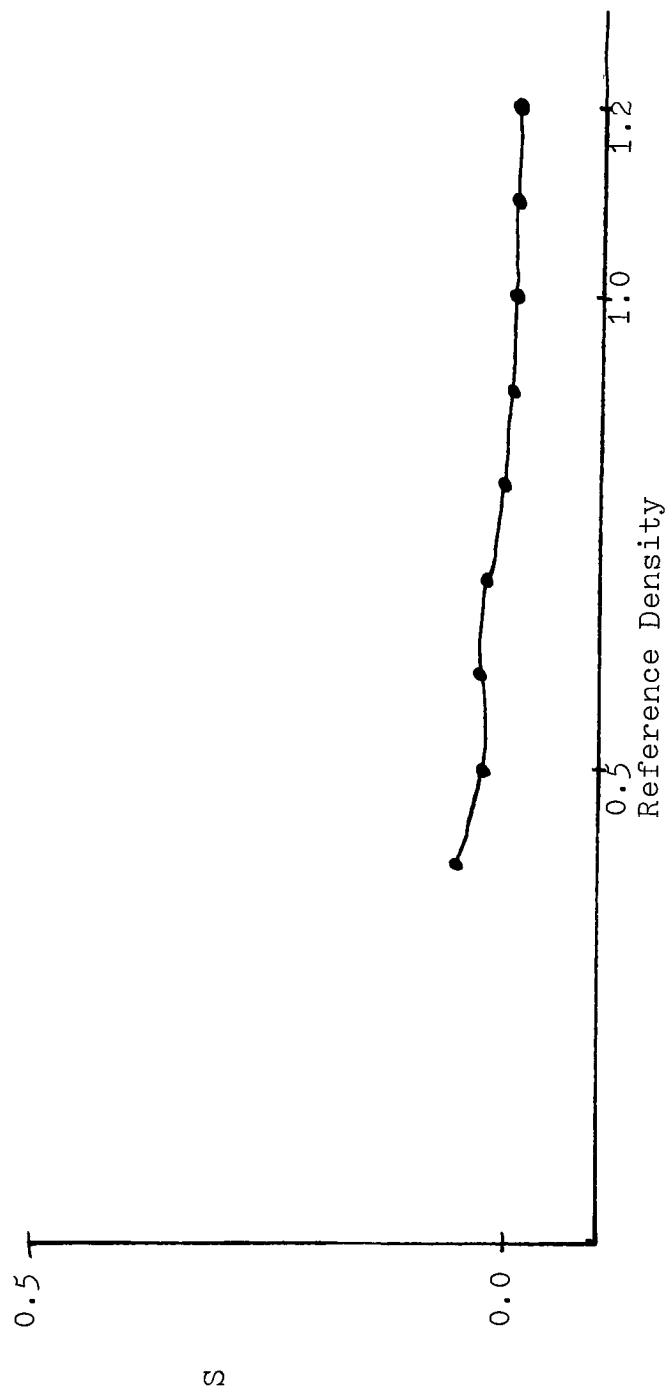


Fig. 24. Superadditivity as a function of Density with supplementary exposure at  $-1.16 \log \text{rel.H}$  corresponding to .20 over  $B+F$

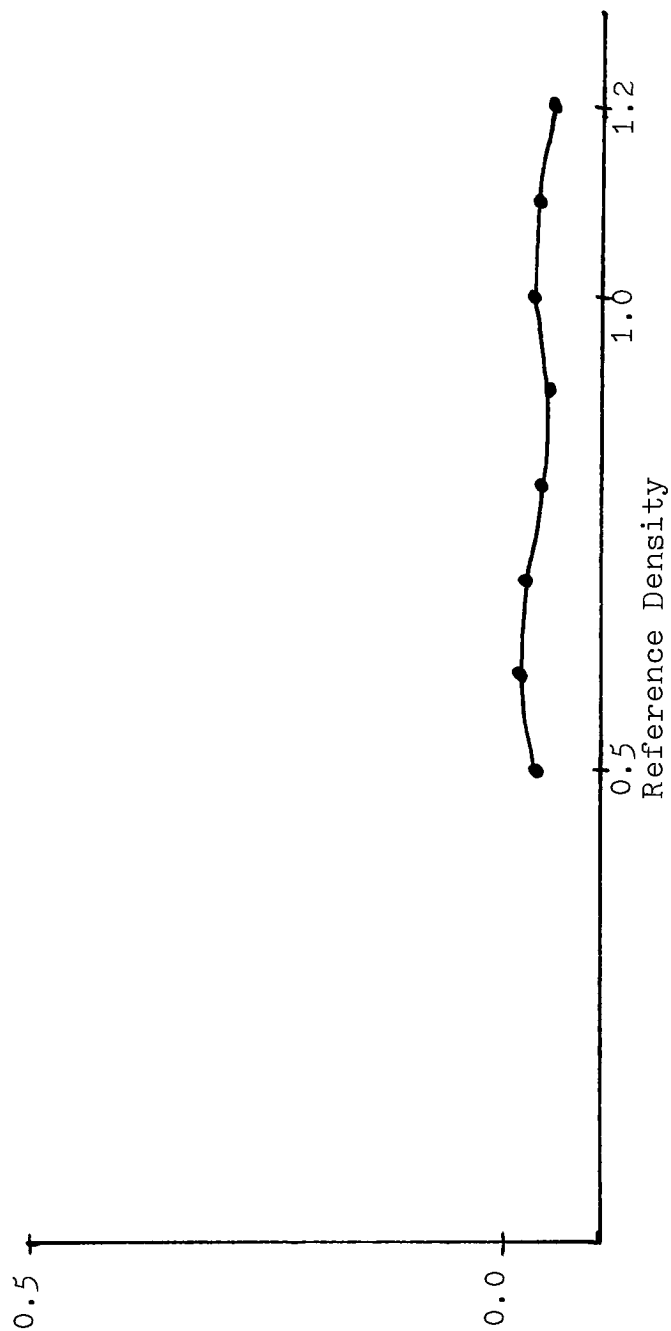


Fig. 25. Superadditivity as a function of Density with supplementary exposure at -1.1 Log rel.H corresponding to .26 over B+F



negative. A positive  $S$  is indicative of superadditivity with respect to exposure. These results are summarized Figures 20 to 25 which represent  $S$  as a function of density, for varying supplementary exposure. The advantage of this format is that  $S$  is directly associated with superadditive speed increases, based upon a 0.30 log exposure shift is equivalent to a one stop change in speed. As with the superadditive density model, the superadditive exposure model indicates the supplementary exposure having a decreasing effect as the shoulder of the characteristic curve is approached. A significant result of this part of the analysis is that CPA can, and indeed does, result in superadditivity with respect to exposure in the toe portion of the characteristic curve.

Regarding optimum IRED intensity, an IRED exposure giving a density of 0.20 above Base + Fog results in the largest values of  $L$  and  $S$ . However, an IRED exposure giving a density of 0.15 over Base + Fog results in greater efficiency in the toe of the curve. At greater supplementary exposure levels, the overall efficiency of the technique decreases. This leads to the hypothesis that there is a decrease in the interstitial silver ion concentration (viz. there are too many electrons in excess) resulting in less than maximum growth activity of the stable sub-image specks. Based upon these results, the IRED exposure giving a density of 0.15 over Base +

Fog was considered optimum for the balance of the testing.

Regarding the speed increases claimed by C&C Research, their calculations were based upon a speedpoint of 0.1 over Base + Fog. Utilizing this criteria, CPA resulted in a speed increase of 1.63 stops being realized with HSIR, which corroborates the claims made by C&C. However, Aerial film speeds are indexed according to a speedpoint of 0.3 over Base + Fog. This criteria only indicates a speed increase of 0.57 stop. It is therefore concluded that this image enhancement technique is not efficient enough to bring High Definition Aerial Infrared materials up to a working speed equivalent to the higher speed materials without any special chemical amplification techniques.

In addition to an unfiltered Xenon flash, CPA was also evaluated when the source was filtered (1) by a Kodak Wratten 12 filter and (2) by a Kodak Wratten 89B filter. The results of this testing, summarized in Figures 26 and 27, were that there were no changes in the efficiency of the technique. These results were expected based upon the work of Moore<sup>17</sup> who arrived at similar conclusions for the case of hypersensitization, where it was determined that hypersensitization doesn't change the film's spectral sensitivity to the source.

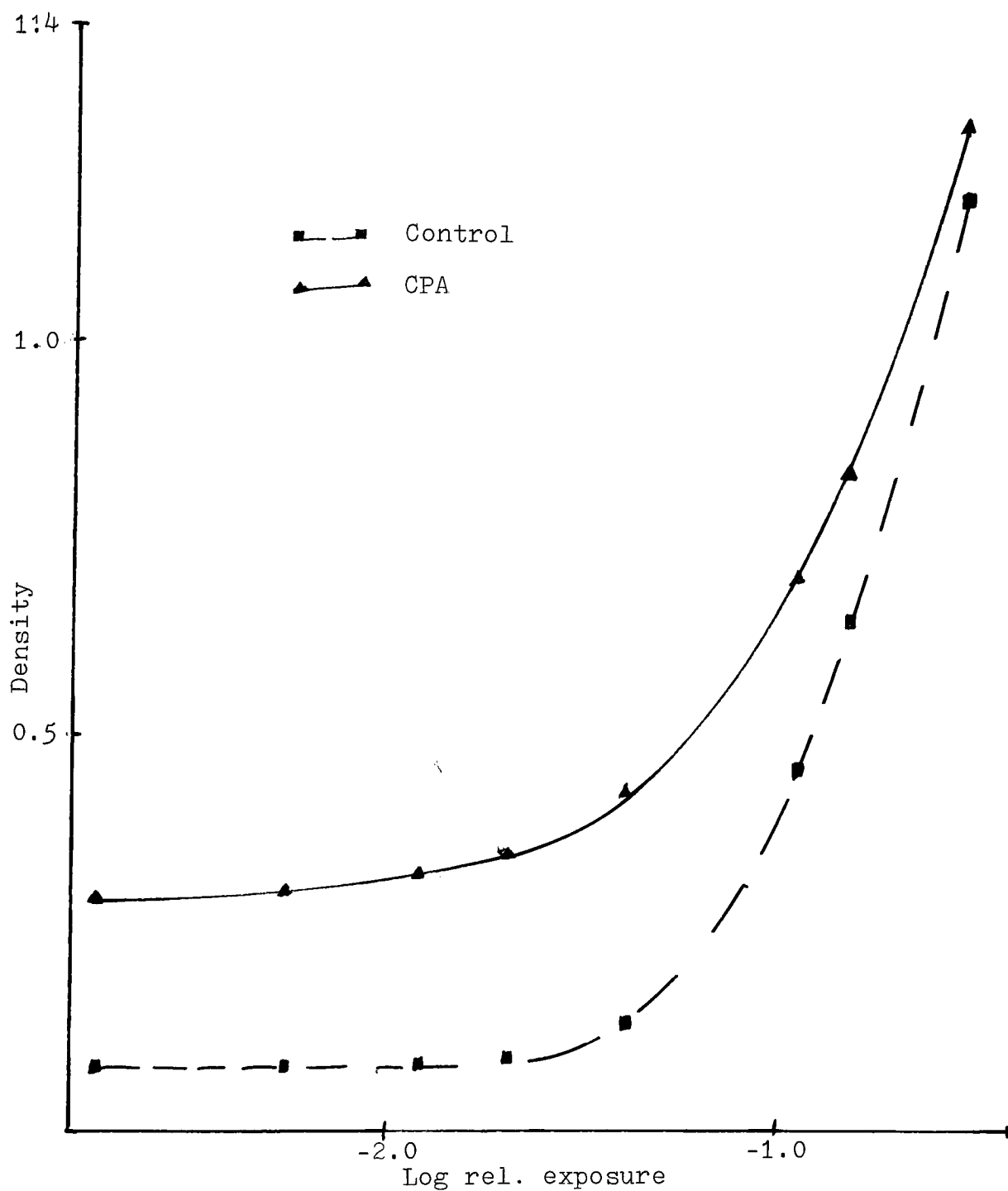


Fig. 26. Density as a function of exposure. Imaging exposure made through a Kodak Wratten 12 filter.

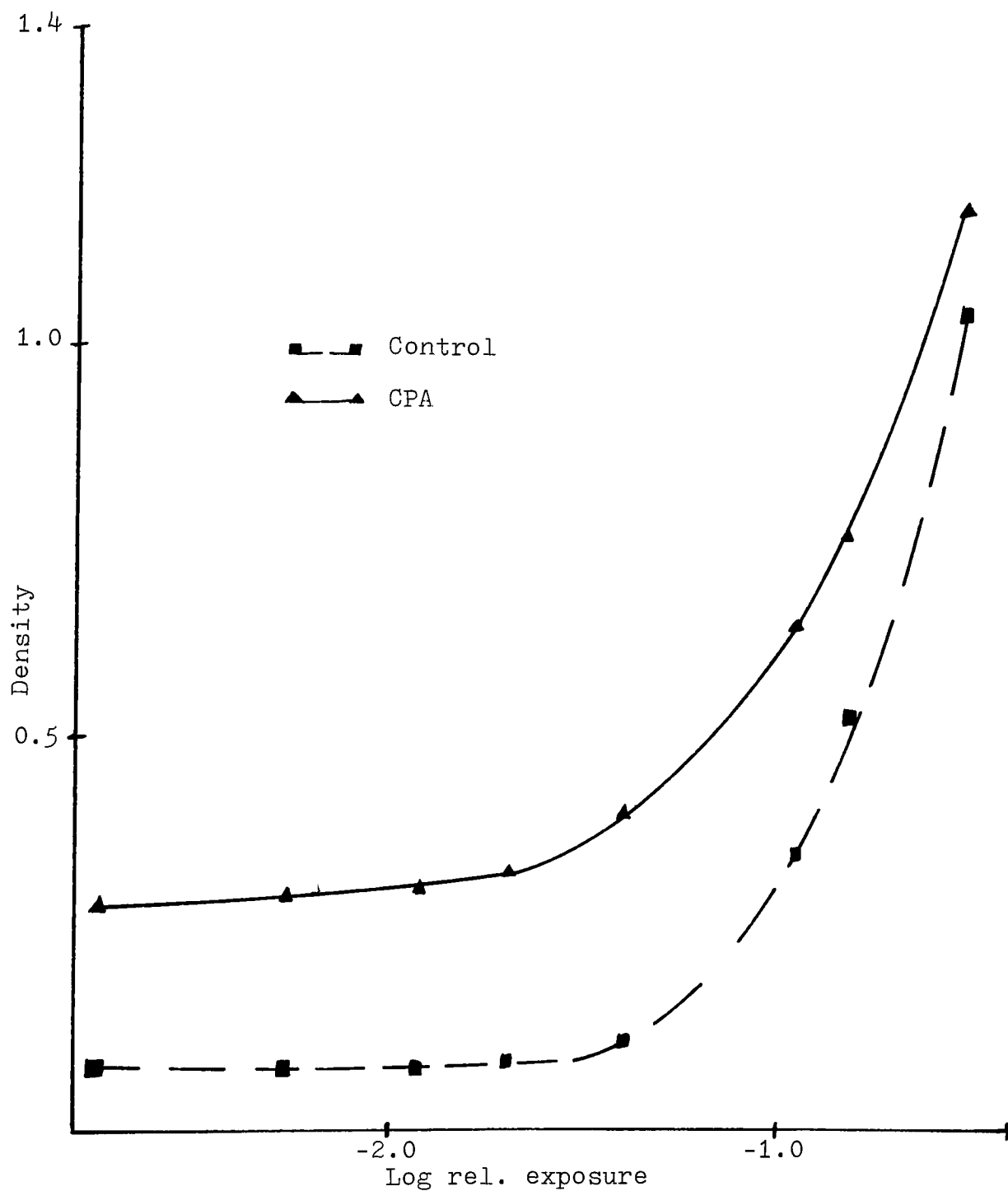
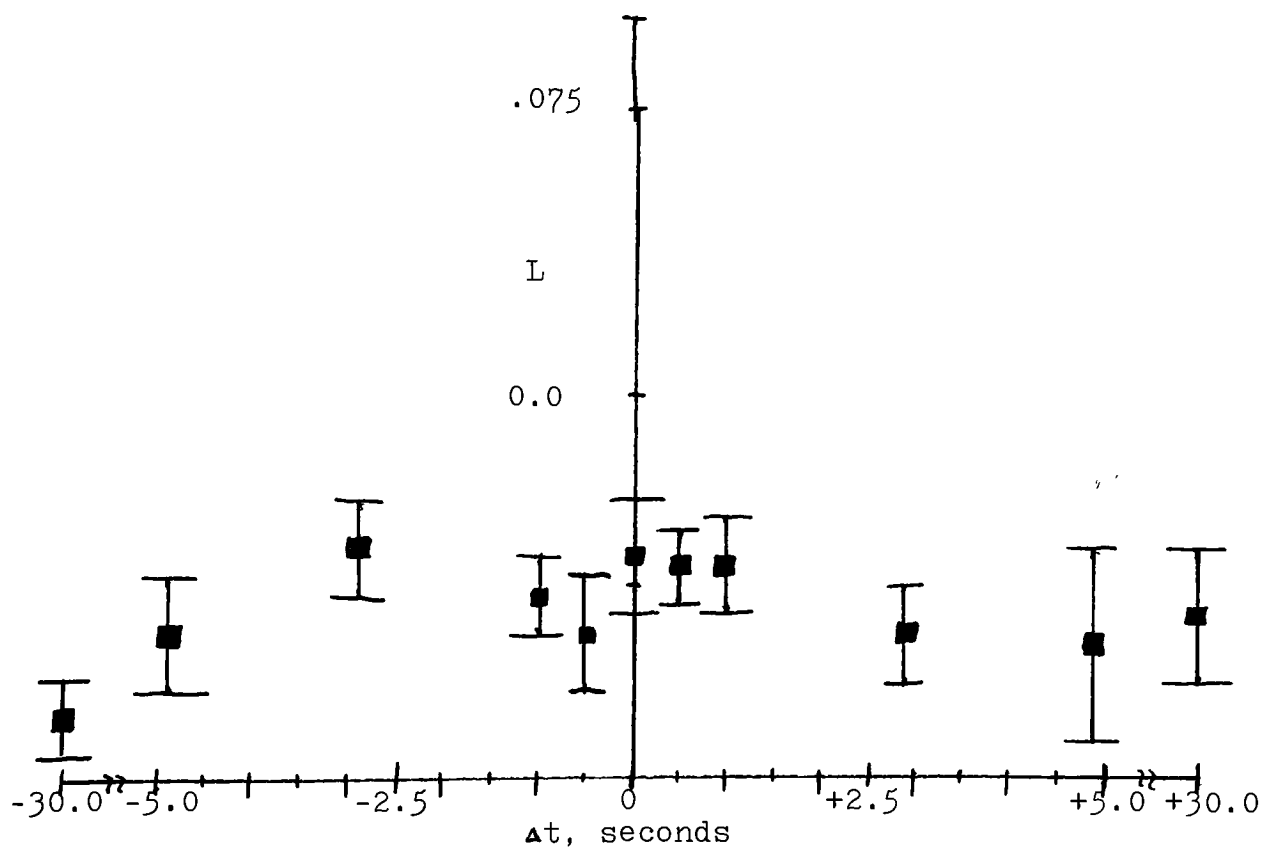
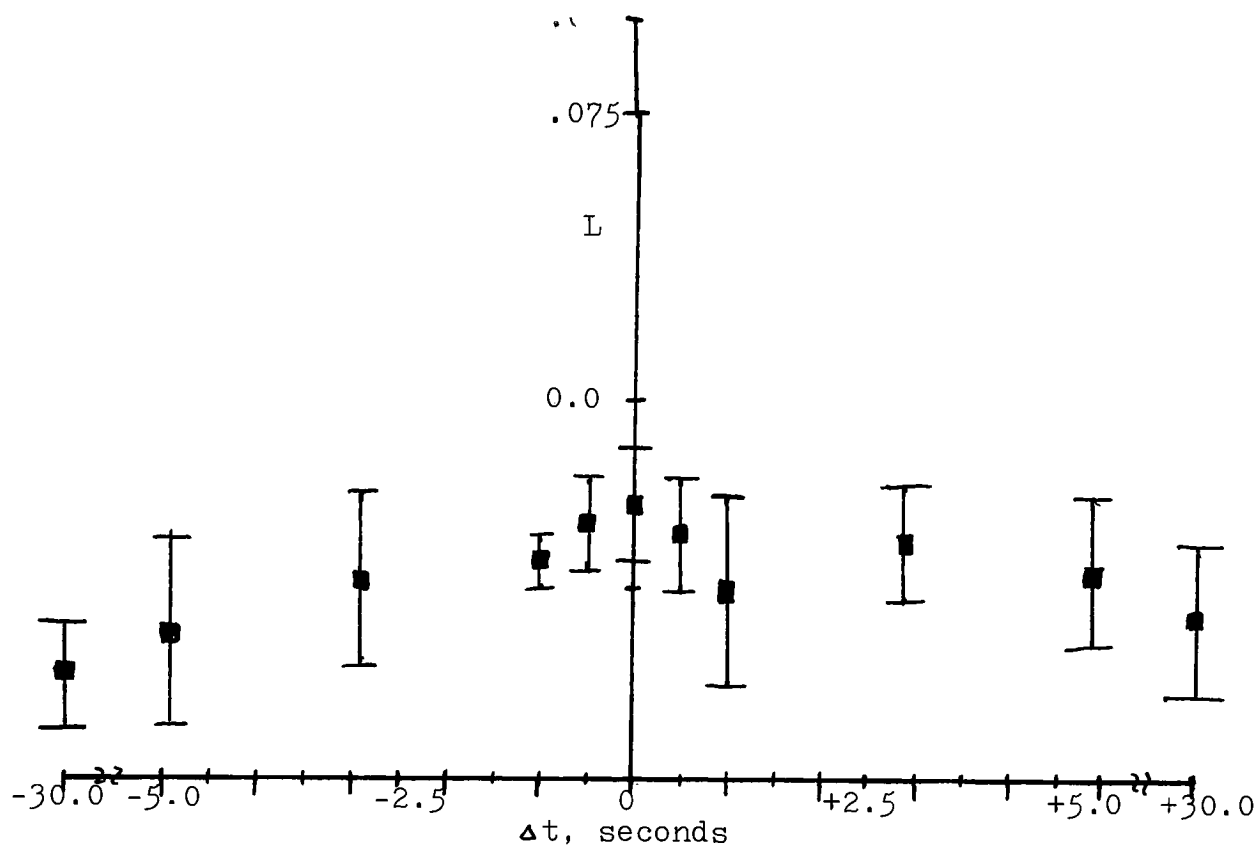


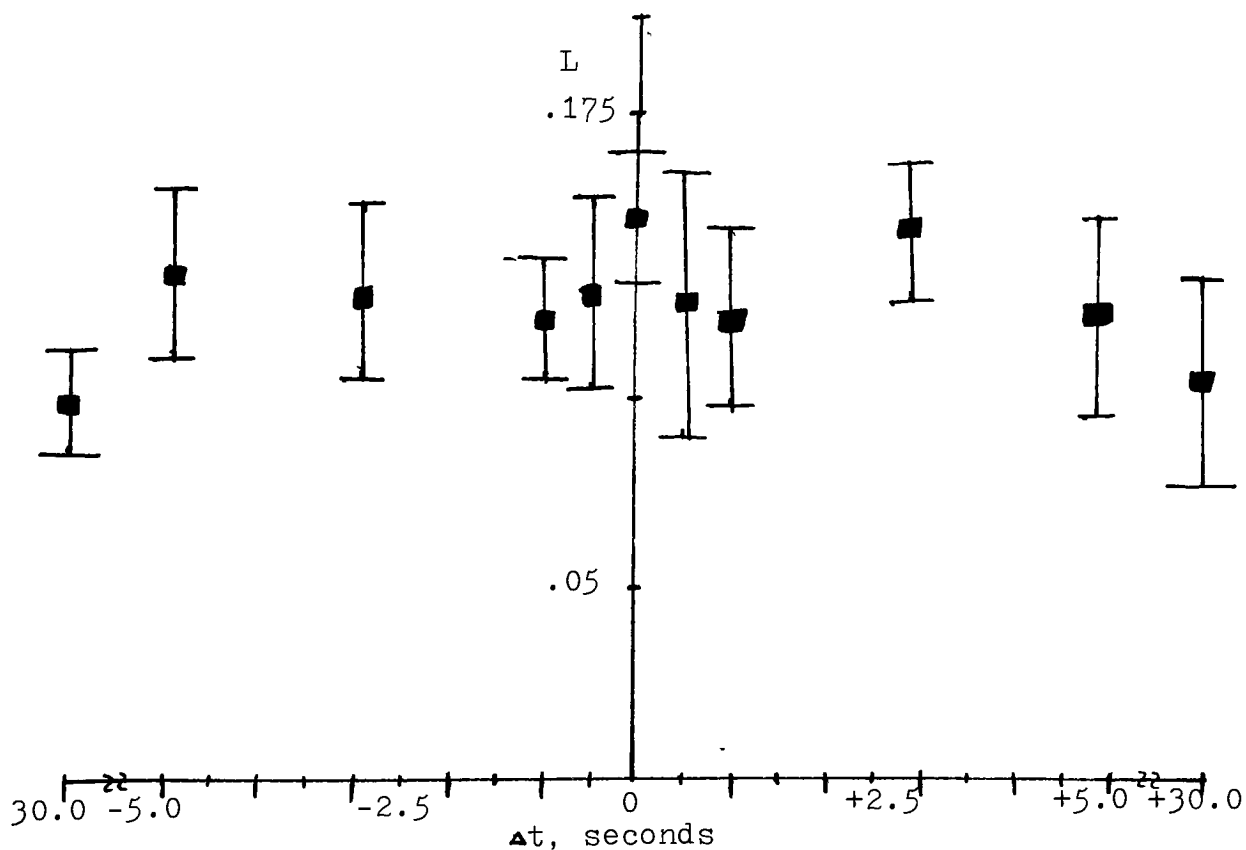
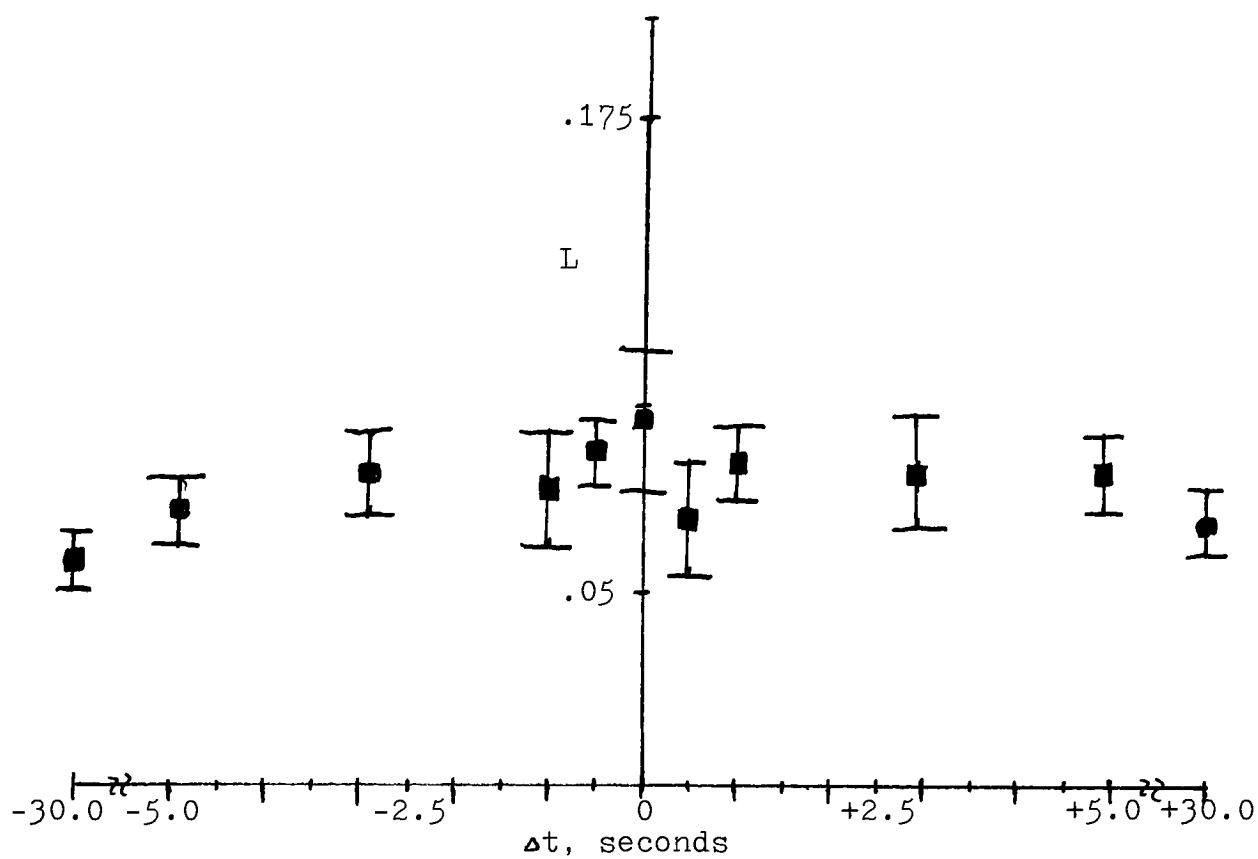
Fig. 27. Density as a function of exposure. Imaging exposure made through a Kodak Wratten 89B filter

In the comparison of CPA with hypersensitization and latensification,  $L$  was the response variable considered. The results are summarized in Figures 28-35, representing  $L$  as a function of  $\Delta t$ , the relative time difference between imaging and supplementary exposures. This time difference ranged from -5 seconds (hypersensitization) to +5 seconds (latensification), in addition to  $\pm 30$  seconds. In every case, the supplementary exposure was fixed to give a density of .15 over Base + Fog. The final results indicated that there was no significant difference (alpha risk of 0.05) between the three image enhancement techniques with dark intervals up to five seconds. It is therefore inferred from these results that while CPA is efficient at "growing" the sub-specks to a developable size, the 0.1 second supplementary exposure time is too short to provide for the chance formation of full specks. It is felt that this is indicative of a shortcoming of CPA: the efficiency of CPA is limited by the fact that the supplementary exposure is limited to a maximum equal to the imaging exposure time, in comparison to latensification which has no such restriction on the supplementary exposure time.

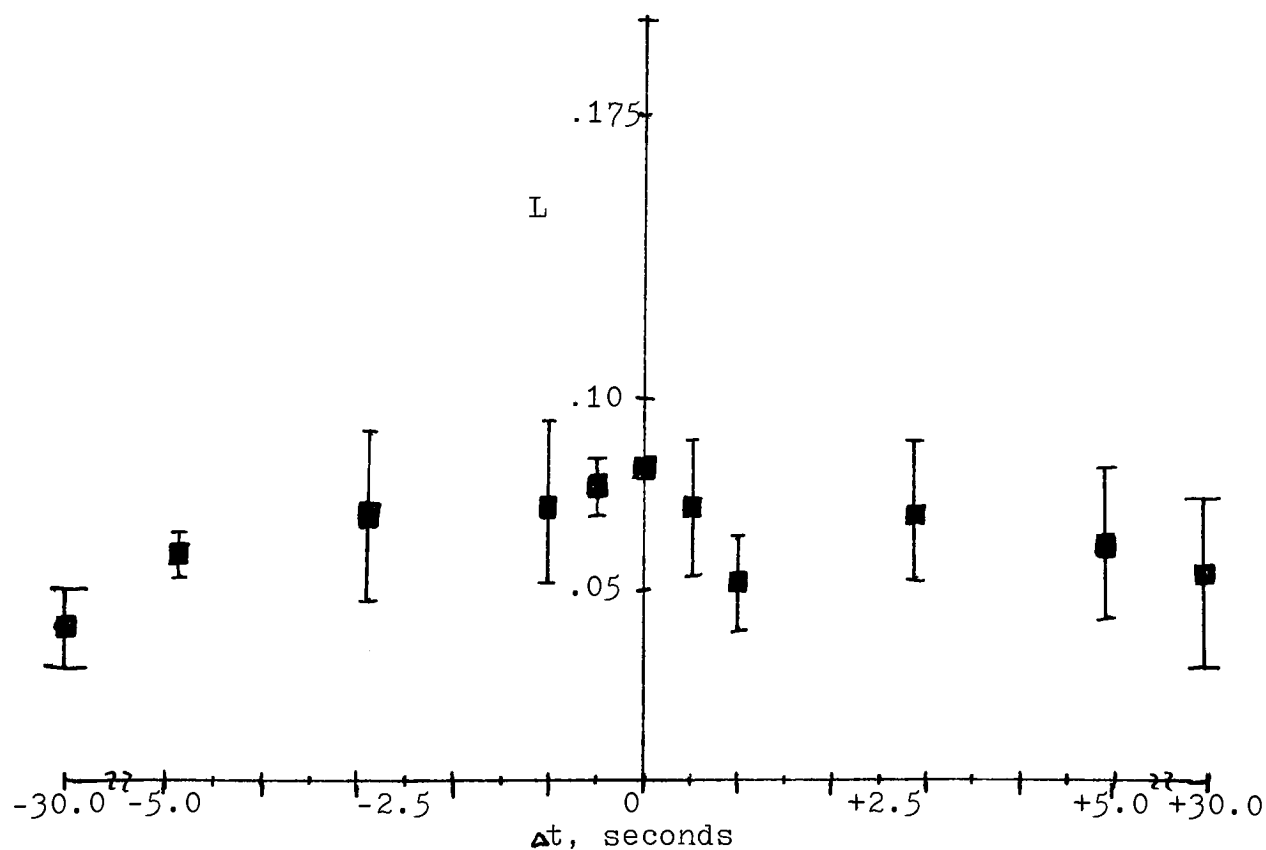
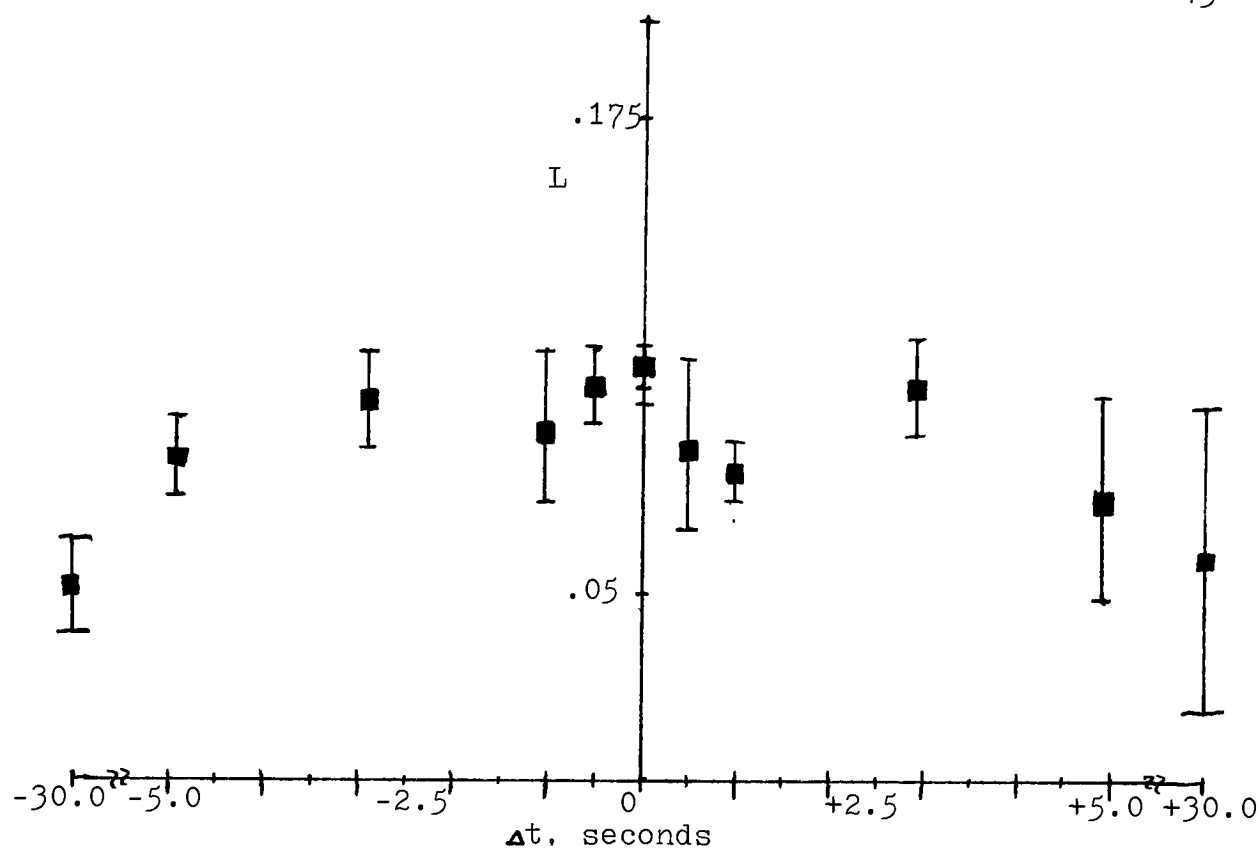
The non-significant difference of hypersensitization with CPA and latensification is accounted to the IRED intensity being at a level such that the growth rate may be slightly higher than the recombination rate. To confirm this theory,



Figs. 28(top) and 29(bottom) . Superadditivity as a function of dark interval. Imaging exposures at  $-0.53 \text{ Log rel.H}$ (top) and  $-0.82 \text{ Log rel.H}$ (bottom)

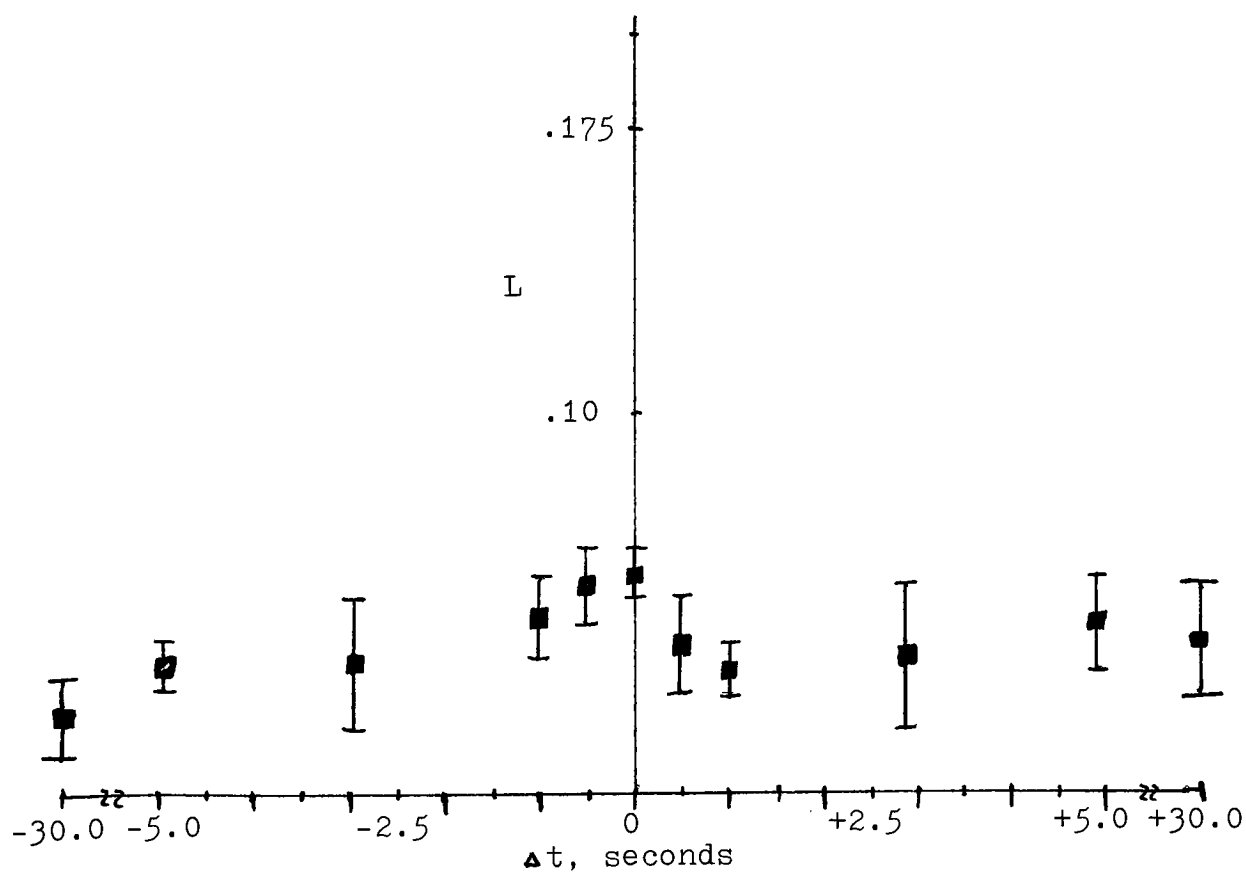
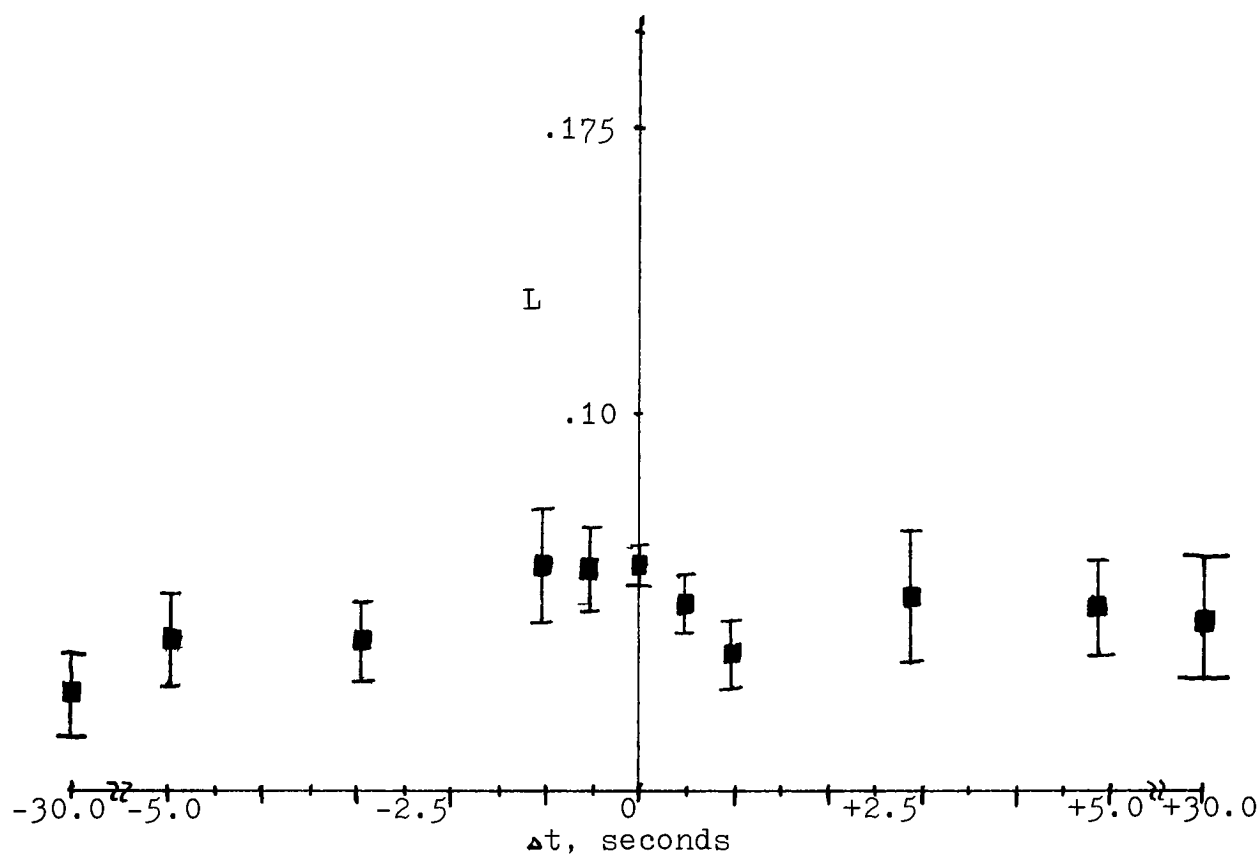


Figs. 30(top) and 31(bottom). Superadditivity as a function of dark interval. Imaging exposures at  $-0.95 \text{ Log rel.H}$ (top) and  $-1.39 \text{ Log rel.H}$ (bottom)



Figs. 32(top) and 33(bottom). Superadditivity as a function of dark interval. Imaging exposures at  $-1.70 \text{ Log. rel.H}$ (top) and  $-1.92 \text{ Log. rel.H}$ (bottom)





Figs. 34(top) and 35(bottom). Superadditivity as a function of dark interval. Imaging exposures at  $-2.26 \text{ Log rel.H}$ (top) and  $-2.74 \text{ Log rel.H}$ (bottom)

hypersensitization and latensification were examined with  $\Delta t$  equal to thirty seconds. As figures 28-35 illustrate, there was no significant change in the latensification case as compared with the previous data. This is only a confirmation of Burton's and Berg's conclusion<sup>18</sup> that latensification just brings the sub-specks to a developable size. In the case of hypersensitization with a thirty second dark interval, there is a significant decrease in the efficiency of the technique. While this can be taken as a confirmation of the above stated proposal, one would also be tempted to draw inferences about the state of stability of the grains during the latent-image formation process. This move will be resisted due to the lack of supporting data regarding hypersensitization with dark intervals ranging from five to thirty seconds. It is felt that this is a point that does warrant further investigation. This portion of the study does not in the least suggest contradiction of the results of Webb & EVans, Burton & Berg, and others. The 0.1 second supplementary exposure time used in this study differed (viz. was less than) from that in the previous work by up to four orders of magnitude.

### CONCLUSION

In summary, it is seen that Concurrent Photon Amplification (CPA) results in superadditive density. That is, the density resulting from concurrent application of imaging and supplementary exposure is greater than the sum of the densities produced by the same exposures when applied separately. This effect appears most pronounced in the region of the characteristic curve where the toe breaks into the straight - line portion. The efficiency of this technique diminishes as the shoulder of the curve is approached. Furthermore, it was determined that CPA also results in superadditivity with respect to exposure in the toe portion of the characteristic curve, with decreasing effect as the shoulder is approached.

In comparing CPA with hypersensitization and latensification enhancement techniques at 0.1 second supplementary exposure times, it was found that the three techniques did not significantly differ in efficiency for dark intervals ranging up to five seconds. Increasing the dark interval to thirty seconds demonstrated no significant effect on the efficiency of latensification, while there was a significant decrease in efficiency of hypersensitization.

When the imaging source was filtered by a Kodak Wratten 12 or Kodak Wratten 89B filter, there were no significant changes in the efficiency of CPA in comparison to an unfiltered imaging source.

Finally, while the CPA image enhancement technique does demonstrate superadditivity, the technique is not efficient enough to effectively allow for exposure of high definition infrared materials at speed indices equivalent to the higher working speed materials.

LIST OF  
REFERENCES

LIST OF REFERENCES

1. Rome Air Development Center Technical Report RADC-TR-76-151
2. SPIE Vol. 79(1976) Aerial Reconnaissance Systems: KS-128 Night Photo System Flight Test Results.
3. P.C. Burton and W.F. Berg, Photographic Journal, 86B, 2 (1946).
4. ibid.
5. Webb and Evans, Photographic Journal, 80, 188, (1940).
6. Hartree and Hill, J. of Sci. Instr., 9, 329, (1932).
7. Alter, Barber and Edwards, Monthly Notices Roy. Astronom. Soc., 100, 529, (1940).
8. Burton and Berg, Photographic Journal, 86B, 2 (1946).
9. Burton and Berg, Photographic Journal, 86B, 24 (1946).
10. Burton and Berg, Photographic Journal, 86B, 3 (1946).
11. Burton and Berg, Photographic Journal, 86B, 2 (1946).
12. film data in appendix.
13. personal communication with B.H. Carroll.
14. personal communication with R. Francis.
15. An-agitator design in Dave Porter's Masters Thesis, unpublished at this writing.
16. Burton and Berg, Photographic Journal, 86B, 2 (1946).
17. Moore, Photographic Journal, 81, 27, (1941).
18. Burton and Berg, Photographic Journal, 86B, 24 (1946).

## APPENDIX ^A

APPENDIX A -

## Hewlett-Packard HEMT-6000 IRED Operating Characteristics

Description	Value
Radiant Intensity along Mechanical Axis	250 uW/sr
Peak Wavelength (Range)	690-715 nm
Spectral Shift Temperature Coefficient	.193 nm/°C
Output Rise Time (10%-90%)	70 ns
Output Fall Time (90%-10%)	1.5 V

Figure 36 illustrates Relative Intensity versus Wavelength with and without the diffusant applied to the IRED.



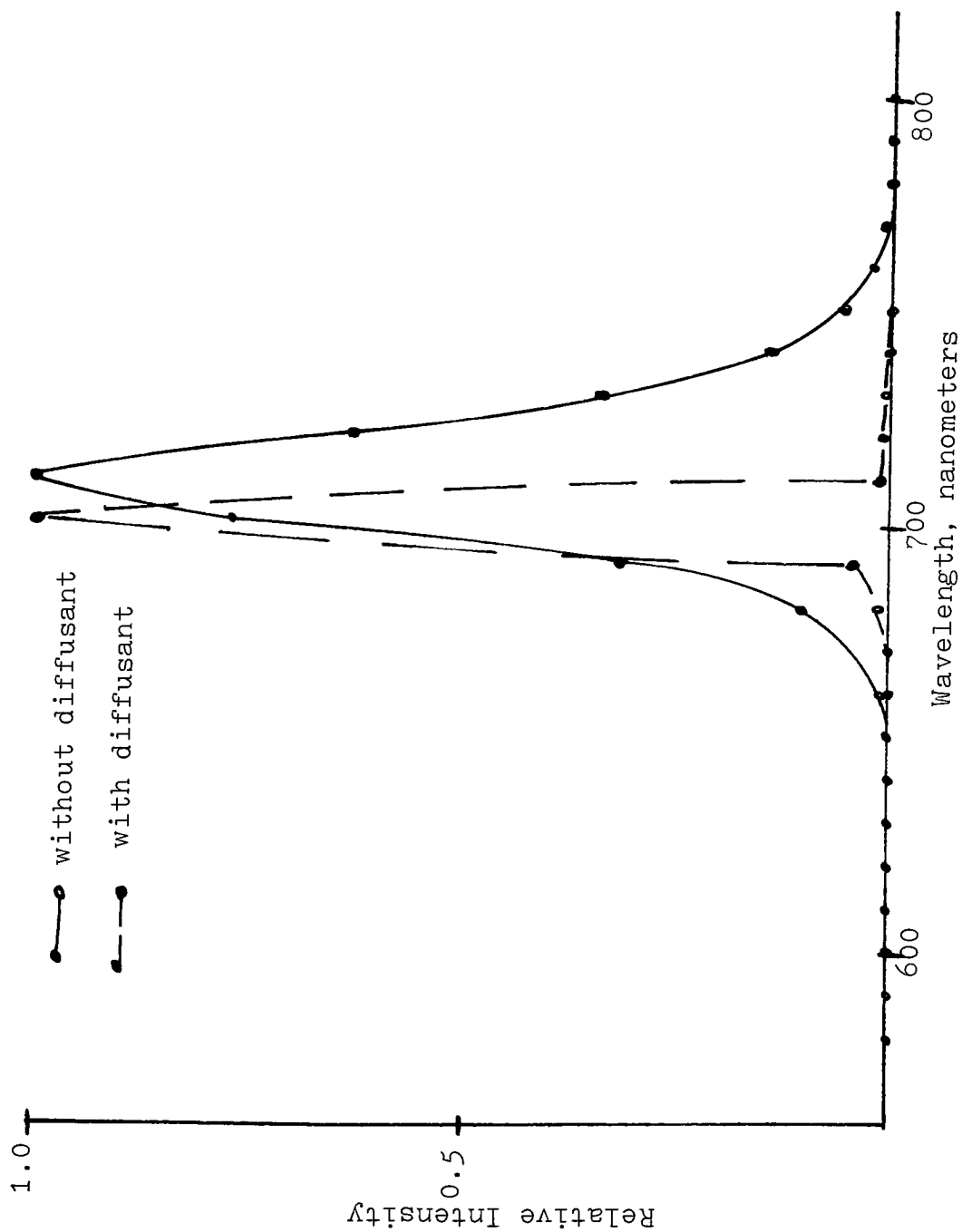


Fig. 36. Relative Intensity versus Wavelength of HEWT-6000 IRED

## APPENDIX B

APPENDIX B

## Film and Processing Data

Film type: Kodak High Speed Infrared  
Emulsion Batch #2481 119

Agitation: Continuous Tumble Activity @ 30 tumbles/minute

Processing: D-19 6 minutes @ 68°F  
Stop Acetic Acid 1 minute @ 68°F  
Fix Kodak F-5 Fixer 10 minutes @ 68°F  
Wash 30 seconds Running Water  
Kodak Hypo Clear 2 minutes @ 68°F  
5 minutes Running Water  
Rinse Kodak Photo-Flo 30 seconds

## APPENDIX C

APPENDIX C

## Electronic Circuit Component Values

$R_1, R_5$  - 5 MegOhm variable resistor  
 $R_2, R_4, R_6$  - 10K,  $\frac{1}{2}$  watt resistor  
 $R_3$  - 100K variable resistor  
 $R_7$  - 200K variable resistor  
 $R_{8-13}$  - 500 Ohm trimmer resistor  
 $R_{14}$  - 270K, 1 watt resistor  
 $R_{15}$  - 100K, 1 watt resistor  
 $R_{16,17}$  - 50 Ohm, 10 watt resistor  
 $R_{18}$  - 2 Ohm, 5 watt resistor  
 $R_{19}$  - 150K, 2 watt resistor  
 $R_{20}$  - 3.3K, 2 watt resistor  
 $C_{1,4,7}$  - 100uF, 25 V electrolytic capacitor  
 $C_{2,5,8}$  - .01uF disk ceramic capacitor  
 $C_{3,6}$  - .001uF disk ceramic capacitor  
 $C_9$  - 1.0uF, 200 V capacitor  
 $C_{10}$  - 250 pF, 600 V capacitor  
 $C_{11}$  - 250uF, 475 V electrolytic capacitor  
 $C_{12}$  - 10uF, 600 V capacitor  
 $D_1$  - 1N914 Diode  
 $D_{2-7}$  - HEMT-6000 IRED's  
 $D_{8-11}$  - 2.5 A, 1000 V Diode  
 $L_1$  - 155 uH choke